



UNIVERSITY OF LEEDS

This is a repository copy of *Basin analysis using seismic interpretation as tools to examine the extent of a basin ore 'play'*.

White Rose Research Online URL for this paper:

<https://eprints.whiterose.ac.uk/164000/>

Version: Accepted Version

Article:

Jenkins, AP and Torvela, T orcid.org/0000-0003-1539-8755 (2020) Basin analysis using seismic interpretation as tools to examine the extent of a basin ore 'play'. *Ore Geology Reviews*, 125. 103698. ISSN 0169-1368

<https://doi.org/10.1016/j.oregeorev.2020.103698>

© 2020, Elsevier. This manuscript version is made available under the CC-BY-NC-ND 4.0 license <http://creativecommons.org/licenses/by-nc-nd/4.0/>.

Reuse

This article is distributed under the terms of the Creative Commons Attribution-NonCommercial-NoDerivs (CC BY-NC-ND) licence. This licence only allows you to download this work and share it with others as long as you credit the authors, but you can't change the article in any way or use it commercially. More information and the full terms of the licence here: <https://creativecommons.org/licenses/>

Takedown

If you consider content in White Rose Research Online to be in breach of UK law, please notify us by emailing eprints@whiterose.ac.uk including the URL of the record and the reason for the withdrawal request.



eprints@whiterose.ac.uk
<https://eprints.whiterose.ac.uk/>

1
2
3
4 **1 Basin analysis using seismic interpretation as tools to examine the extent of a basin**
5 **2 ore 'play'**
6
7
8
9

10 4 Alexander P. Jenkins^{1,2}, Taija Torvela^{1*}

11 5 ¹Ores and Mineralisation Group, University of Leeds, School of Earth and Environment, Leeds,
12 6 LS2 9JT, UK

13 7 ²University of Bristol, School of Earth Sciences, Bristol, BS8 1RJ, UK

14 8 APJ: <https://orcid.org/0000-0001-6396-0402>

15 9 TT: <https://orcid.org/0000-0003-1539-8755>

16 10 * Correspondence (T.M.Torvela@leeds.ac.uk)
17
18
19
20
21
22
23
24

25 12 Keywords: Pb-Zn; seismic reflection data; basin ores; basin analysis; normal faults; fault timing
26
27
28

29 14 **Abstract**

30
31 15 Stratiform and stratabound base metal ores typically form in sedimentary basins during the
32
33 16 overall rifting process with mineralising fluids transported along the growing normal faults.
34
35 17 Understanding the detailed structural evolution, i.e. the timing, the growth and the extent of
36
37 18 the faults, and the distribution and thickness of the syn-faulting sedimentary packages, is
38
39 19 critical for focusing exploration efforts. In this paper, we describe how seismic interpretation
40
41 20 and basin analysis techniques can help to do this. We assess the potential for Pb-Zn
42
43 21 mineralisation within the Northumberland Trough, northern England, in the context of the wider
44
45 22 Early Carboniferous basin evolution and the associated base metal ores. Through structural
46
47 23 interpretation of seismic reflection data, we consider the detailed evolution of the fault
48
49 24 geometries and sedimentation in time and space, to show the extent and distribution of the
50
51 25 Early Carboniferous faulting and growth packages at depth in the study area. We conclude
52
53 26 that basin evolution and structural framework in northern England is very similar to that
54
55 27 associated with the significant Pb-Zn mineralisation in Ireland. We suggest a refined model for
56
57
58
59

60
61
62
63
64
65
66
67
68
69
70
71
72
73
74
75
76
77
78
79
80
81
82
83
84
85
86
87
88
89
90
91
92
93
94
95
96
97
98
99
100
101
102
103
104
105
106
107
108
109
110
111
112
113
114
115
116
117
118

28 the Carboniferous evolution of this part of the basin. The study demonstrates how the
29 techniques of basin analysis can be a used in ore exploration to establish whether the basic
30 structural and sedimentary framework exists to enable mineralisation. In addition to assessing
31 the general potential of base metal mineralisation, a more precise identification of potentially
32 suitable areas for further investigation can be made. The seismic data and basin analysis
33 approach used in this paper and exemplified through the Northumberland case should be
34 directly applicable to any basin ore 'play' associated with rifting and/or sedimentation. The
35 added, significant advantage of this method is the ability to assess the 3D fault geometries,
36 including fault linkage and growth in space and time, and the associated sedimentation - an
37 unachievable outcome if relying solely on other geophysical and geological data traditionally
38 used in regional ore exploration.

119
120
121 **1. Introduction**
122

123 41 In hydrocarbons exploration, the concept of a 'play' is routinely used to refer to a group of
124 42 prospects in a region that are controlled by the same set of geological circumstances. Detailed
125 43 understanding of these circumstances is key for effective exploration. A number of techniques
126 44 can be used to analyze plays, but robust understanding of the structural and depositional
127 45 evolution of the region in time and space always underpins more detailed prospect targeting.
128 46 For sedimentary basins, seismic reflection data interpretation is the most commonly used tool
129 47 for to establish the fundamental structural and depositional framework: it is widely used in
130 48 hydrocarbons exploration (e.g. Jackson and Beales, 1967; Miklereit et al., 1996; Hu et al.,
131 49 2017); but also, increasingly, in basin ore exploration and research (Gibson et al., 2016;
132 50 Ashton et al., 2018). Crucially, seismic interpretation and basin analysis allow establish the
133 51 timing of fault activity and the extent of syn-kinematic (syn-rift) sedimentation by observing
134 52 and interpreting the thickness increase towards the fault in the sedimentary packages (Fig.
135 53 1A-C). In this paper, we demonstrate the usage of the technique of basin analysis through
136 54 seismic reflection interpretation in the context of basin ores exploration. We establish the
137 55 timing and structure of a Carboniferous basin in Northern England, showing that the faulting
138 56 event is of similar nature and timing compared to that associated with the significant base
139 57 metal mineralisation in Ireland. The method presented here is a powerful tool, especially in
140 58 the early phases of exploration outwards from a known deposit where it is necessary to
141 59 investigate the extent of the play: i.e. whether the overall timing and the structure of a basin
142 60 and the faults and sedimentary packages within it are suitable for mineralisation in the regional
143 61 context.

144 62 The Early Carboniferous lead-zinc play in Ireland is well known with its >25 economic and
145 63 subeconomic deposits and has been extensively studied (e.g. Max et al., 1983; Taylor, 1984;
146 64 Hitzman and Large, 1986; Williams et al., 1986; Anderson et al., 1988; Shearley et al., 1992;
147 65 Hitzman and Beaty, 1996; Everett et al., 1999; Hitzman, 1999; Lewis and Couples, 1999;
148 66 O'Reilly et al., 1999; Wilkinson, 2010; Ashton et al., 2015; Wilkinson & Hitzman 2015;
149 67 Torremans et al., 2018; Kyne et al., 2019). Significant mineralisation exists at Tynagh,

178
179
180 68 Silvermines, Lisheen, and at Navan, the latter being a world-class Pb-Zn deposit (Fig. 2).
181
182 69 Recently, a 2D seismic survey helped to identify the Tara Deep satellite deposit at Navan
183
184 70 which is now under development (Ashton et al., 2018). The mineralisation is normally
185
186 71 classified as 'Irish type', which is thought to be a hybrid between Mississippi Valley type (MVT)
187
188 72 and SEDEX ores (e.g. Torremans et al., 2018) although some authors consider the Irish type
189
190 73 to be a sub-type of the MVT deposits (e.g. Leach et al., 2001). Whatever the detailed
191
192 74 classification may be, the key observations for the purposes of this paper are that the Irish
193
194 75 mineralisation i) occurs as stratabound replacement ore within the Lower Carboniferous pre-
195
196 76 to syn-rift carbonate sequences present across the Irish Midlands basin; and ii) is closely
197
198 77 associated with major normal faults which acted as main fluid conduits (e.g. Ashton et al, 2015,
199
200 78 2018; Wilkinson & Hitzman 2015; Torremans et al., 2018; Kyne et al., 2019).

201
202 79 Lateral equivalents of the Lower Carboniferous rocks in Ireland are exposed in
203
204 80 northernmost England and southwestern Scotland, particularly in the Northumberland Trough
205
206 81 and on the upfaulted Alston Block (Fig. 2). The potential for Carboniferous lead-zinc
207
208 82 mineralisation in the Northumberland Trough has not been studied in detail although the
209
210 83 possibility has been suggested (e.g. Plant et al., 1988; Jones et al. 1994; Chadwick et al. 1995;
211
212 84 Walsh et al. 2018; Baba et al., 2019). Most of the known mineralisation in the area is related
213
214 85 to the so-called Northern Pennine Orefield (NPO), with historically mined zinc ores (Figs. 2,
215
216 86 3). The known NPO mineralisation is not of the 'Irish type'; it is around 50 Ma younger
217
218 87 (Permian), located structurally higher, and is associated mostly with fractures and fissures
219
220 88 within the bedding rather than being a strictly stratabound replacement ore (Fig. 3; e.g. Kimbell
221
222 89 et al. 2010). In the absence of sufficient drilling, the most tangible evidence for an 'Irish type'
223
224 90 Early Carboniferous mineralising event comes from the British Geological Survey Mineral
225
226 91 Reconnaissance Programme: stratabound mineralisation in Lower Carboniferous carbonate
227
228 92 rocks has been found at or close to current exposure levels near normal faults around
229
230 93 Langholm and Saughtree (Fig. 2), along with some fracture-style mineralisation in the volcanic
231
232 94 rocks of the same age and in the Silurian basement (drilling reached depths of ~25 m;
233
234 95 Gallagher et al., 1977; Smith et al., 1996). The indications of base metal mineralisation in the

237
238
239
240
241
242
243
244
245
246
247
248
249
250
251
252
253
254
255
256
257
258
259
260
261
262
263
264
265
266
267
268
269
270
271
272
273
274
275
276
277
278
279
280
281
282
283
284
285
286
287
288
289
290
291
292
293
294
295

96 Lower Carboniferous combined with the regional similarities in the Lower Carboniferous
97 geological history between Ireland and northern England raise the possibility that previously
98 unrecognised rifting-related, 'Irish type' Pb-Zn mineralisation could exist at depth in northern
99 England. For this to be the case, the structural setting including the timing of the major faults
100 and the deposition of thick syn-rift sediments of suitable carbonitic composition need to be
101 similar in northern England to those associated with the Irish Pb-Zn deposits. It is very difficult
102 to decipher fault timings, growth and 3D geometries from surface data alone, but basin
103 analysis techniques can greatly illuminate the overall structural setting (Fig. 1). We apply such
104 techniques through interpretation of a grid of 2D seismic lines within the Northumberland
105 Trough, in order to establish the structural setting and evaluate its similarity to the Irish Pb-Zn
106 play. Our analysis incorporates the timing of the major faulting, fault geometries and linkage
107 during growth, and the thickness and distribution of the syn-kinematic sediments in the area -
108 both crucial for the presence of ores similar to the Irish deposits. We discuss the results in the
109 context of Pb-Zn mineralisation in Ireland to propose a refined model for how the main
110 structures within the study area may host mineralisation at depth, therefore potentially
111 extending the lead-zinc play into northern England and southwestern Scotland; the presence
112 of suitable host rock lithologies at depth, however, remains to be tested by drilling. The method
113 used in this paper, exemplified through the Northumberland case, should be directly applicable
114 to any basin-related ore deposit associated with faulting and/or sedimentation.

115

116 **2. Geological Context**

117 Any basin analysis must be underpinned by robust understanding of the regional geological
118 evolution and local stratigraphy. Therefore, we first summarize the geological history of the
119 British Isles and Ireland during the Carboniferous, focusing on the structural context of the Pb-
120 Zn mineralisation in Ireland and northern England and on the stratigraphy of the study area.

121 *2.1 Geological History*

296
297
298
299
300
301
302
303
304
305
306
307
308
309
310
311
312
313
314
315
316
317
318
319
320
321
322
323
324
325
326
327
328
329
330
331
332
333
334
335
336
337
338
339
340
341
342
343
344
345
346
347
348
349
350
351
352
353
354

122 The known Pb-Zn mineralisation in the Irish Midlands and in northern England broadly
123 follows the trend of the Iapetus Suture (Fig. 2; Max et al. 1983; Ashton et al. 2015). The suture
124 is a structurally complex region formed by the closure of the Iapetus Ocean and the
125 subsequent continental collision during the Caledonian Orogeny around 400 Ma (Torsvik et
126 al. 1996; McKerrow et al. 2000; Stone et al. 2010). The dominantly NE-SW Caledonian
127 structural grain controlled the overall trend of the Carboniferous syn-rift faults with which the
128 Irish base metal mineralisation is genetically related (O'Reilly et al. 1999; Ashton et al. 2015;
129 Torremans et al. 2018; Kyne et al., 2019). The Carboniferous rifting was caused by
130 approximately north-south orientated tension, probably due to back-arc extension caused by
131 the northward subduction of the Rheic Ocean beneath the southern margin of the Caledonian
132 basement (Leeder, 1982; Nance et al. 2012). The major basin produced by this north-south
133 divergence extends from both northern England to the Irish Midlands and is characterised by
134 fault-bound blocks separated by deep sub-basins (Leeder 1982; Hitzman 1999). In northern
135 England, faulting localisation was also controlled by granitic Caledonian plutons in the Lake
136 District, the North Pennines and the Cheviots (Fig. 2); these acted as rigid bodies during the
137 extension, forming structural highs or horst blocks (Stone et al., 2010). Subsidence history
138 analysis in northern England shows the initial rapid fault-controlled subsidence (rift phase)
139 during the Tournaisian-Visean was followed by gradually declining regional subsidence (sag
140 phase) from the late-Visean to Westphalian (McKenzie, 1978; Kimbell et al., 1989).

141 The ENE-WSW trending Northumberland Trough - Solway Basin occupies the generally
142 low-lying land between the Solway Firth and Northumbrian coast (Fig. 2). To the south, the
143 basin margin follows the prominent highs of the Lake District and Alston (North Pennine)
144 Blocks along the Maryport-Stublick-Ninety Fathom fault system. This north-dipping normal
145 fault system was initiated in the Tournaisian and early Visean, resulting in a thick Lower
146 Carboniferous syn-rift sequence accumulating in the Northumberland-Solway Basin and partly
147 outcropping in the northern part of the basin (Chadwick et al., 1995). The northern margin of
148 the Northumberland-Solway Basin is formed by en-échelon, mostly south-dipping faults,
149 antithetic to the Maryport-Stublick-Ninety Fathom faults. The throw on the northern basin-

355
356
357 150 bounding fault system increases westwards, resulting in the Solway Basin having a roughly
358
359 151 symmetrical shape in cross section, whilst the Northumberland Trough approximates a half-
360
361 152 graben (Chadwick et al. 1995). However, the detailed timings and geometries of individual
362
363 153 faults and sedimentary packages remain largely unknown.

365 154 Subsidence ceased by the latest Carboniferous and was replaced with the peripheral
366
367 155 effects of the Variscan Orogeny around 290 Ma (Matte, 1986; Collier, 1989; Stone et al.,
368
369 156 2010). Variscan deformation in northern England is identified by deformation affecting the
370
371 157 Westphalian Coal Measures but not the overlying Permian strata. Variscan structures in
372
373 158 northern England include gentle folding, minor thrusting/inversion, and removal of up to 2 km
374
375 159 of Carboniferous sediment due to uplift and erosion (Chadwick et al., 1995). Some authors
376
377 160 suggest that the inversion structures result from transtensional tectonics rather than Variscan
378
379 161 compression (De Paola et al., 2005). Intrusion of the Permian Whin Sill complex at 297 Ma
380
381 162 and other broadly coeval intrusions (Figs. 3 and 4) post-date the inversion, but pre-date a
382
383 163 Permian extensional or transtensional event (Collier, 1989; Dempsey, 2016).

384
385 164

386 165 *2.2 Stratigraphy of Northumberland*

388 166 The metamorphosed Lower Paleozoic basement in northern England is unconformably
389
390 167 overlain by some Devonian, but mostly Carboniferous rocks (Fig. 4). The late Devonian – early
391
392 168 Carboniferous crops out sporadically along the northern margin of the Northumberland
393
394 169 Trough; these semi-arid fluvial beds have been described as pre-rift (Leeder, 1973; 1974) or
395
396 170 earliest syn-rift (Chadwick and Holliday, 1991). The main rift basin succession is of
397
398 171 Carboniferous age, controlled by the evolving normal fault system (Fig. 5; e.g. Dunham, 1990;
399
400 172 Chadwick et al., 1995). The syn-rift packages are exposed in the north but buried in the
401
402 173 southern part of the basin (Fig. 4). The region is characterised by the general absence of syn-
403
404 174 rift sediments from horst tops such as the Alston Block (Fig. 5; Stone et al., 2010). By the end
405
406 175 of the Viséan, active rifting ceased, allowing Asbian and younger strata to progressively
407
408 176 accumulate across the area (Bott et al., 1984; Kimbell et al., 1989).

414
415
416 177 The syn-rift Courceyan to Chadian age Inverclyde Group rocks are, where observed at
417
418 178 outcrop or in boreholes, mainly siliciclastic fluvial to shallow marine sediments, but fine-grained
419
420 179 carbonates as nodules and thin beds are also common (Stone et al., 2010). Basaltic lavas are
421
422 180 present in this group, at least along the NW margin of the Trough, and are interpreted as
423
424 181 marking the onset of rifting (Leeder, 1974). The Border Group forms the main syn-rift basin fill
425
426 182 of up to 4 km of fluvial to marine siliciclastic and carbonate rocks (Dunham, 1990). Where
427
428 183 exposed (in the north), the dominant rock types especially higher in this group are composed
429
430 184 of the fluvial Fell Sandstones, but grade into deltaic then marine conditions towards the south
431
432 185 and west (Johnson, 1980). The exposed parts of the Lyne Formation (in NE Northumberland
433
434 186 Trough) contain some clastic and nonmarine limestones interpreted as peritidal with
435
436 187 increasingly marine limestone layers higher in the succession (Dean et al., 2011). The rock
437
438 188 types within the Border Group at depth in the deeper parts of the basin remain unknown as
439
440 189 there are few historic drill holes and they mostly reach depths of only a few hundred metres.
441
442 190 Evaporite layers present in the Border Group may be important for mineralisation as a potential
443
444 191 source of saline fluids (Day, 1970) but also as potential top-seal to control lateral fluid migration
445
446 192 (see discussion). Either way, the Inverclyde Group and the Border Group are the
447
448 193 approximately time-equivalent sequences in northern England to the sediments hosting the
449
450 194 Irish Pb-Zn deposits (Fig. 4).

451 195 Late Viséan and Namurian rocks of northern England mainly belong to the Yoredale Group.
452
453 196 Yoredale facies is characterised by cyclothems of marine limestone overlain by shale,
454
455 197 sandstone, and coal (Hudson, 1924; Stone et al., 2010). The early Asbian Tyne Limestone
456
457 198 Formation of the Yoredale Group displays greater marine influence than the exposed parts of
458
459 199 the underlying Border Group but maintains alternating marine input from the SW and clastic
460
461 200 input from the NE (Leeder et al., 1989). Approximately coevally with the Tyne Limestone
462
463 201 Formation, a thin (~100 m) sequence of non-Yoredale ramp to shelf carbonates belonging to
464
465 202 the Great Scar Limestone Group was deposited on the structurally elevated Alston Block
466
467 203 (Stone et al., 2010). By the end of the Asbian, a marine transgression during the regional sag
468
469 204 phase covered all of the Alston Block and the Yoredale facies Alston and Stainmore

473
474
475
476
477
478
479
480
481
482
483
484
485
486
487
488
489
490
491
492
493
494
495
496
497
498
499
500
501
502
503
504
505
506
507
508
509
510
511
512
513
514
515
516
517
518
519
520
521
522
523
524
525
526
527
528
529
530
531

205 Formations of the Yoredale Group were deposited across the entire area (Fig. 4; Chadwick et
206 al., 1995). The top of the Alston Formation is marked by the Great Limestone Member, the
207 thickest outcropping limestone in the area at 20 m thickness; this formation hosts a large
208 proportion of the known Permian vein mineralisation (Fig. 3; Dunham, 1990).

209

210 *2.3 Mineralisation: summary of the Irish and NPO lead-zinc ores*

211 We briefly summarize the main characteristics of Irish Pb-Zn mineralisation and the known
212 Pb-Zn mineralisation in the Northern Pennine Orefield (NPO). For a more detailed description
213 of mineralisation and stratigraphy in the NPO, the reader is referred to Dunham (1990), Tucker
214 et al. (2003) and Bott and Smith (2018), and to the BGS Mineral Exploration Programme
215 reports from northern England and southern Scotland (e.g. Smith et al., 1996). For more
216 details on the Irish Carboniferous stratigraphy and Irish base metal mineralisation see e.g.
217 Philcox (1984), Wilkinson and Hitzman (2015), Ashton et al. (2015). Torremans et al. (2018)
218 and Kyne et al. (2019).

219 'Irish-type' mineralisation is a sedimentary rock-hosted ore deposit type in which large-scale
220 normal faults channel mineralising fluids from depth into the host rocks (typically carbonates;
221 Fig. 6). The mineralisation is predominantly epigenetic with respect to deposition of the host
222 lithologies, but syn-kinematic with respect to the rifting process that created the faults,
223 although fluid flow along faults can continue for a time after active faulting has ceased (e.g.
224 Walsh et al., 2018). Irish-type mineralisation overlaps with both the so-called Mississippi Valley
225 type (MVT) mineralisation which usually forms deeper in a (foreland) basin, and with syn-
226 genetic sedimentary-exhalative (SEDEX) ores deposited directly onto the seafloor. Some
227 authors consider the 'Irish-type' to be a sub-type of the MVT (e.g. Leach et al., 2001).
228 Regardless of the debate on the exact deposit 'type', the key observation for the purposes of
229 this paper is that all of the Irish deposits are a) strongly fault-controlled in terms of the fluid
230 pathways into the system; and b) form stratabound ore lenses close to the faults and within
231 the syn-rift stratigraphy.

532
533
534
535
536
537
538
539
540
541
542
543
544
545
546
547
548
549
550
551
552
553
554
555
556
557
558
559
560
561
562
563
564
565
566
567
568
569
570
571
572
573
574
575
576
577
578
579
580
581
582
583
584
585
586
587
588
589
590

232 In Ireland, the faulting patterns related to ore genesis are complex especially in the world-
233 class Navan deposit and its newly discovered Tara Deep satellite deposit (Ashton et al., 2018).
234 Some crucial commonalities can, however, be observed. The main ore-controlling faults are
235 large normal or slightly normal-oblique faults (>100 m throw, at Navan possibly up to >2km;
236 Table 2). They mostly trend NE-SW although smaller faults within relay ramps between the
237 main faults are probably significant: at e.g. Silvermines and Lisheen E-W to NW-SE striking
238 relay-ramp breaching faults are linked to mineralisation (Torremans et al., 2018). The deposits
239 are stratabound to stratiform lenses which thin away from their feeder faults over several
240 hundred metres (e.g. Lewis and Couples, 1999; Torremans et al., 2018; Kyne et al., 2019).
241 The Lower Carboniferous rocks that host mineralisation in the Irish Midlands are a
242 transgressive carbonate sequence of mostly Courceyan age (Hitzman and Large, 1986).
243 Mineralisation is generally found in non-argillaceous carbonates, oolitic limestones, or clean
244 dolostones, usually in the stratigraphically lowest horizon with any of those lithologies present
245 (e.g. Hitzman and Beaty, 1996). In the northern and central Irish Midlands, this is the Meath
246 Formation (informally known as 'Pale Beds') of the Navan Group, deposited as variable
247 shallow water shelf carbonates. South- and southwest-wards, the Navan Group becomes
248 increasingly shale-rich and passes into the Lower Limestone Shale, representing a deepening
249 of the palaeo-basin (Hitzman and Beaty, 1996). Here, mineralisation is found in the
250 stratigraphically higher late Courceyan-Chadian reef limestones of the Feltrim Formation (the
251 'Waulsortian Limestone'; Hitzman and Beaty, 1996). The exact timing of mineralisation is
252 debated but probably occurred <5 Ma after the deposition of the host rocks in most areas,
253 constrained by both isotope evidence and erosion-mineralisation relationships; late Chadian
254 or early Arundian age is likely for the majority of the deposits but mineralisation may have
255 started as early as Courceyan in some areas (Anderson et al., 1998; Ashton et al., 2015).
256 Mineralisation is, in summary, controlled primarily by suitable host lithologies and structures,
257 rather than being constrained to a certain stratigraphic horizon.

258 In the Irish Midlands, deposits occur mostly on the downthrown side of the normal fault
259 segments but footwall ores also exist (Hitzman, 1999; Ashton et al., 2018). Feeder zones to

591
592
593
594
595
596
597
598
599
600
601
602
603
604
605
606
607
608
609
610
611
612
613
614
615
616
617
618
619
620
621
622
623
624
625
626
627
628
629
630
631
632
633
634
635
636
637
638
639
640
641
642
643
644
645
646
647
648
649

260 the orebodies are spatially associated with points of maximum throw on the faults or with
261 deformed (breached) relay ramps (Taylor, 1984; Shearley et al., 1992; Hitzman and Beaty,
262 1996; Torremans et al., 2018; Kyne et al., 2019). At the world-class Navan deposit, most of
263 the mineralisation of the main ore body is concentrated within a highly fractured relay ramp
264 between the two major NW-dipping faults (Ashton et al., 2015, 2018). However, a new satellite
265 deposit, Tara Deep, has been identified deeper in the palaeobasin, SE of a basement horst
266 delimiting the main ore body where it seems to be associated with the footwall of the major
267 basin-bounding Navan Fault with km-scale displacement (Table 2; Ashton et al., 2018).

268 In detail, the genesis of 'Irish-type' ores remains contentious. Most authors agree that
269 mineralisation occurred during or soon after active faulting and involved mixing of deep
270 ('basinal'), high-temperature, acidic, metal-bearing fluids and shallow, low-temperature, high-
271 sulphur, high-salinity brines derived from seawater/basin sediments (Fig. 6; e.g. Wilkinson,
272 2010; Wilkinson and Hitzman, 2015). At Navan, the shallow sulphur-rich fluids were produced
273 by bacterial reduction of Lower Carboniferous seawater, likely in deep half-grabens formed
274 during the rifting (Anderson et al., 1998). Mixing of the two fluids was facilitated by the faults
275 which acted as permeable conduits, focusing fluid flow and allowing episodic tapping of the
276 deep metal-rich fluid reservoir during the faulting cycle (Wilkinson and Hitzman, 2015). The
277 last stages of syn-sedimentary faulting at Navan are interpreted to be Chadian-Arundian,
278 suggesting that the mineralisation occurred <5 Ma after deposition of the host rocks (Hitzman
279 and Beaty, 1996). The exact timing and depth of mineralisation may be variable; there is some
280 evidence for syn-genetic exhalation of minerals (SEDEX-type mineralisation) into seawater in
281 the later, topmost parts of the multi-layered deposit (especially within the so-called 'slide
282 complex'), but most of the ore seems to have formed through deeper epigenetic processes
283 (Ashton et al., 2015; Wilkinson and Hitzman, 2015).

284 In contrast to Irish Midlands, the known (Pb-)Zn mineralisation in northern England is mainly
285 Permian, although indications of possible Carboniferous mineralisation have also been found.
286 The Permian mineralisation is dated at 294 ± 29 Ma by Os-Os dating (Dempsey 2016) and at
287 292 ± 20 Ma by U-Pb dating (Dunham, 1990). It occurs mainly within a thin Carboniferous

650
651
652 288 sequence on the Alston Block, deposited in baryte-fluorite veins with some strata-bound,
653
654 289 mineralised wall rock replacement (alteration) zones (Fig. 3; Table 1; e.g. Bouch et al., 2006).
655
656 290 Significant mineralisation also occurs within the Alston Formation in the southern
657
658 291 Northumberland Trough, north of the Stublick Fault (Fig. 3; e.g. Dunham, 1988; Kimbell et al.,
659
660 292 2010). In terms of Carboniferous mineralisation, BGS surveys near Langholm and Saughtree
661
662 293 (Fig. 2) revealed stratabound sphalerite, occurring as replacement minerals in dolomitic vugs
663
664 294 in the exposed Lower Carboniferous carbonate rocks, and also found a number of Zn and Ba
665
666 295 anomalies during stream sediment heavy concentrate sampling (Gallagher et al., 1977; Smith
667
668 296 et al., 1996). Other, indirect evidence comes from a regional panning programme in the
669
670 297 southern and eastern parts of the Northumberland Trough which revealed significant lead,
671
672 298 zinc, and copper anomalies in stream sediments where Lower Carboniferous sediments are
673
674 299 exposed (Bateson et al., 1983).

675 300 Both the Irish Midlands and the NPO are highly prospective areas for Pb-Zn mineralisation.
676
677 301 Although Early Carboniferous Irish-type deposits have not been found in Northern England,
678
679 302 the possibility is apparent from; i) the existence of the major normal fault systems associated
680
681 303 with Carboniferous rifting; ii) the projection of mineral-bounding lineaments in Ireland across
682
683 304 the Irish Sea into northern England; iii) the presence of suitable carbonate-bearing host-rocks
684
685 305 of similar Lower Carboniferous age in both areas (Jones et al., 1994). The discovered
686
687 306 stratabound sulphide mineralisation in Lower Carboniferous rocks in northern England and
688
689 307 southwestern Scotland indeed point towards a functioning base metal deposition system
690
691 308 during Lower Carboniferous (Gallagher et al., 1977; Smith et al., 1996). In order to establish
692
693 309 whether Irish-style ores may have developed in northern England, we need a better
694
695 310 understanding of the timing, geometry and extent of Early Carboniferous faulting along with
696
697 311 the extent of and thickness variations within the syn-rift sedimentary packages. Basin analysis
698
699 312 techniques utilising seismic reflection data interpretation can be used to test whether this Early
700
701 313 Carboniferous favourable structural framework exists in northern England (Fig. 1).

702
703 314

705 315 **3. Data and methods**

709
710
711 316 The principal method was interpretation of seismic reflection data, assisted by borehole data,
712
713 317 following the standard approach described in e.g. Gerhardstein and Brown (1984) and in Fig.
714
715 318 1. The seismic reflection lines were provided in standard SEG-Y format by the UK Onshore
716
717 319 Geophysical Library (UKOGL; see www.ukogl.org.uk for their interactive seismic line viewer).
718
719 320 All seismic lines used are time-migrated 2D land surveys (i.e. the vertical extent is expressed
720
721 321 in seconds Two-Way Travel time, TWT, rather than in metres), shot throughout the 1980's
722
723 322 using Vibroseis sources. The quality of the dataset is highly variable. Given the range of
724
725 323 vintages, processing parameters, and need for static corrections in land surveying, small mis-
726
727 324 ties between surveys do occur. Despite the quality variations, several lines provide a good
728
729 325 overview of the geometries of the basement and the interpreted basin infill horizons, clearly
730
731 326 picking out the main features and giving a reasonable estimate of the sub-surface structure
732
733 327 and fault configuration as per the procedure outlined in Fig. 1. The available lines were ranked
734
735 328 based on quality, the ranking subsequently informing the geological interpretation in terms of
736
737 329 uncertainty assessment; the poorest quality lines were not interpreted.

738
739 330 Basic information of several boreholes, often with both formation tops and time-depth
740
741 331 charts, are available at the UKOGL library. Two boreholes, Longhorsley-1 and Stonehaugh,
742
743 332 are located within the study area and these were used to assist interpretation of the seismic
744
745 333 data (Fig. 4). The Stonehaugh borehole penetrates down to the Fell Sandstone Formation
746
747 334 (601 m total length), whilst Longhorsley-1 reaches the upper part of the underlying Lyne
748
749 335 Formation at 1829 m in the shallower parts of the basin. This leaves a large thickness ($>>1$
750
751 336 km) of basin sediment unsampled, especially within the deeper parts of the basin, leaving their
752
753 337 character unknown. British Geological Survey 1:50000 scale digital surface geology mapping
754
755 338 provided an indication of the outcrop pattern of the main formation boundaries and the
756
757 339 locations of the main fault structures. The geological maps give the rock types associated with
758
759 340 each formation at outcrop, but their lateral facies changes at depth towards the south and west
760
761 341 remain unknown. The top of the Early Carboniferous Fell Sandstone Formation of the Border
762
763 342 Group has outcrop control in the far NW of the study area and is the only horizon that can be
764
765 343 tied to both boreholes. The Tyne Limestone and Alston formations of the overlying Yoredale
766
767

768
769
770
771
772
773
774
775
776
777
778
779
780
781
782
783
784
785
786
787
788
789
790
791
792
793
794
795
796
797
798
799
800
801
802
803
804
805
806
807
808
809
810
811
812
813
814
815
816
817
818
819
820
821
822
823
824
825
826

344 Group are present in the Longhorsley-1 well only, although both have extensive outcrop
345 control to the south and east.

346 Structural interpretation was performed using IHS Kingdom suite seismic interpretation
347 software. Borehole formation tops and seismic surveys are referenced to mean sea level
348 (MSL) datum; this is given in the processing information for some but not all vintage lines. Of
349 the available UKOGL seismic dataset, only those surveys with sufficient quality to be useful
350 were used in interpretation; their traces are shown in Figure 4. Fixing minor mis-ties between
351 surveys (<0.05 s TWT) was considered impractical for the purposes of this study, considering
352 that the required time shift may vary along each survey due to static corrections in land
353 surveying. Boreholes helped to constrain the main contacts (Top Lower Groups, Top Tyne
354 Limestone Fm., and Top Alston Fm.; Fig. 5). An approximate Top Basement was also
355 interpreted, identified by the deepest recognisable coherent reflectors underlain by featureless
356 seismic signal (Fig. 8). Seismic interpretation was performed using the loop tying method so
357 that any inconsistencies and mis-ties could be identified and corrected (see e.g. Gerhardstein
358 and Brown, 1984 for details). The presence of mis-ties meant that in some lines the estimated
359 depths to the interpreted horizons had to be adjusted manually during loop-tying (exemplified
360 by the offset of the Top Basement in Fig. 8). Faults were identified with reference to the surface
361 geological maps and correlation polygons were used to identify the location of the sedimentary
362 horizons across faults, although the result was not always without a degree of uncertainty.
363 Sedimentary horizons were not extrapolated across the basin-bounding faults (the Stublick
364 Fault and Ninety Fathom Fault) due to difficulty identifying suitable reflectors on their footwall
365 and the knowledge that syn-rift formations are likely to be largely absent beyond the basin
366 (Stone et al., 2010; Fig. 5).

367 3D (2.5D) interpretations in the form of structure maps with fault polygons were produced
368 for the interpreted horizons (Fig. 9). The maps were produced using the Flex Gridding
369 algorithm in Kingdom Suite and a grid size of 100 m. Isochron maps for the intervals defined
370 by the interpreted horizons were also produced from the horizon grids in order to approximate
371 the TWT thicknesses of the interpreted packages (Fig. 10).

827
828
829 372 A degree of epistemic uncertainty is inherent in all seismic interpretation. The purpose of
830
831 373 this study is to interpret the general features such as the sedimentary package architecture in
832
833 374 relation to the main faults. We consider the quality of the used lines to be sufficient as these
834
835 375 main structural features are mostly fairly clearly imaged. The greatest cause for uncertainty in
836
837 376 the interpretation arose from assessing the magnitude of displacement across faults where
838
839 377 there is no nearby well or outcrop control, or where mis-ties between lines occur (e.g. such as
840
841 378 in Fig. 8). Using correlation polygons (reflection pattern mis-matches) mitigates the issue
842
843 379 somewhat, although variable data quality is an issue especially in the west part of the area.
844
845 380 Therefore, misinterpretation of up to ~0.05 s TWT should be considered when analysing the
846
847 381 structure maps and the thickness maps (see next section). The surface geology map and the
848
849 382 two boreholes greatly help to constrain the locations of the horizons across faults so that the
850
851 383 main geometries of the faults and the syn-rift packages, and their relationships, can be
852
853 384 interpreted with reasonable certainty.
854
855 385

856 386 **4. Results**

857 387 *4.1 Seismic reflection interpretation*

858
859 388 The representative seismic lines and their interpretations in Figure 8 show the general features
860
861 389 of the results. Three main sedimentary packages were interpreted within the study area: the
862
863 390 'Lower Groups' (delimited by Top Basement and Top Fell Sandstone), the Tyne Limestone
864
865 391 Formation, and the Alston Formation (Fig. 5).

868 392 The Lower Groups package consists of the Border Group and Inverclyde Group with
869
870 393 undefined relative thicknesses. These units are grouped together because, due to the lack of
871
872 394 well control penetrating the deeper units, the Top Fell Sandstone Formation (top of the Border
873
874 395 Group) is the deepest known horizon which can be reliably interpreted in the sub-surface. The
875
876 396 total thickness of the Lower Groups approaches 2 s TWT towards the west (Fig. 8B).
877
878 397 Depending on the seismic velocity of the rocks (typically 2500-4000 m s⁻¹ for sedimentary
879
880 398 rocks) this represents at least 2.5 km, but probably well over 3 km, of basin sediment about
881
882 399 which very little is known (see Kimbell et al., 1989 who estimate that the velocities may be up
883
884
885

886
887
888
889
890
891
892
893
894
895
896
897
898
899
900
901
902
903
904
905
906
907
908
909
910
911
912
913
914
915
916
917
918
919
920
921
922
923
924
925
926
927
928
929
930
931
932
933
934
935
936
937
938
939
940
941
942
943
944

400 to 4500 m s⁻¹ within the basin). The dataset allows some interpretation of the internal
401 geometries within the Lower Groups (yellow dashed lines in Fig. 8. There are some distinctly
402 wedge-shaped geometries present especially in the lower parts of this succession; these are
403 especially evident on the strike sections as exemplified in Fig. 8B. Indications of significant
404 acoustic impedance changes that would be expected from a layered sandstone-mudstone-
405 limestone sequence do occur, such as the prominent high amplitude reflectors found at the
406 base of the succession and locally towards the middle (e.g. around 0.8 ms TWT in Fig. 8B).
407 An area of noticeably lower amplitudes with sometimes chaotic reflectors occurs towards the
408 base of the succession (e.g. around c. 1.4-1.5 s TWT in the west part of Fig. 8B); the cause
409 for these is unknown but they could be caused by evaporites known to be present elsewhere
410 within the Inverclyde Group. The transition from coherent reflectors to featureless seismic
411 signal at depth is interpreted to mark the Top Basement composed of the metamorphosed
412 Caledonian rocks.

413 The Top Tyne Limestone Formation and the overlying Top Alston Formation are interpreted
414 above the Lower Groups (Fig. 8). The Tyne Limestone Formation contains some very high
415 amplitude reflectors; again, the cause of these is unclear but they possibly represent contacts
416 of limestone beds developed due to the increasing marine influence on this formation. The
417 Alston Formation is characterised by lower amplitude, higher frequency reflectors than the
418 underlying formations. The rocks above the Alston Formation belong to the Namurian
419 Stainmore Formation, locally overlain by the Westphalian Coal Measures.

420 From the horizon interpretations, it can be observed that both the Top Basement and the
421 sedimentary succession reflections dip southwards into the Stublick fault hanging-wall (Fig.
422 8A). Near the Stublick Fault, especially the sedimentary successions above the Lower Groups
423 form a broad syncline, with the reflections shallowing out before dipping slightly northwards in
424 the immediate vicinity of the fault. The Lower Groups thicken significantly southwards towards
425 the Stublick Fault and are therefore broadly interpreted as the syn-rift package. The Tyne
426 Limestone Formation appears to thin slightly towards the Stublick Fault, whereas the Alston
427 Formation maintains approximately constant thickness; these formations can thus be broadly

945
946
947
948
949
950
951
952
953
954
955
956
957
958
959
960
961
962
963
964
965
966
967
968
969
970
971
972
973
974
975
976
977
978
979
980
981
982
983
984
985
986
987
988
989
990
991
992
993
994
995
996
997
998
999
1000
1001
1002
1003

428 classified as post-rift. The wedge-shaped geometry of the interpreted syn-rift Lower Groups
429 succession is even clearer in the E-W direction (Fig. 8B); a west-dipping Top Basement is
430 overlain by the syn-rift Lower Groups which display an obvious thickening towards the west,
431 roughly parallel to the strike to the Stublick Fault. However, this strike-section shows more
432 clearly that the topmost part of the Lower Groups show approximately even thickness and
433 may thus be post-rift. The Tyne Limestone Formation thickness seems to remain
434 approximately constant in the E-W direction.

435 All identified faults are normal faults, with approximate throws ranging from the lower limit
436 of vertical seismic resolution (around 20-60 m for these surveys) to possibly up to 2 km. Some
437 faults show weak positive inversion expressed by features such as the anticline between the
438 synthetic-antithetic fault pair in Figure 8A and the hanging-wall anticline in Figure 8B. Both of
439 these anticlines affect the post-rift packages, constraining the maximum age of the folding to
440 Middle Carboniferous. The seismic sections in Figure 8 are vertically exaggerated, which
441 steepens the overall apparent fault dip, although the dip for many large faults appears to
442 shallow out slightly with depth. More faults are identified on north-south sections than east-
443 west sections, due to the dominantly E-W to ENE-WSW strikes of the faults.

444 The Stublick Fault dips northwards and is the longest fault and the largest in terms of
445 displacement. Horizons generally cannot be followed across to its foot-wall, although the Top
446 Basement is interpreted, with some uncertainty, to be displaced by up to 1 s TWT (2 km using
447 an average velocity of 4000 m s⁻¹ for the hanging wall rocks). Interpreted major splays of the
448 Stublick fault are common (Fig. 8A). Overall, the displacement clearly increases towards the
449 west along this major fault zone as indicated by the wedge-shaped growth geometries of the
450 Lower Groups.

451 The Antonstown Fault and Sweethope Fault are examples of other major (>200 m throw)
452 faults. These are found north of the Stublick Fault and show south- and north-ward dips
453 respectively. Both faults can be interpreted to penetrate down into the basement and they may
454 be linked to form a flower structure across the relay zone between these faults (Fig. 8A).

1004
1005
1006
1007
1008
1009
1010
1011
1012
1013
1014
1015
1016
1017
1018
1019
1020
1021
1022
1023
1024
1025
1026
1027
1028
1029
1030
1031
1032
1033
1034
1035
1036
1037
1038
1039
1040
1041
1042
1043
1044
1045
1046
1047
1048
1049
1050
1051
1052
1053
1054
1055
1056
1057
1058
1059
1060
1061
1062

455 Further north- and south-dipping faults with throws of around 100 m or less are frequent in the
456 interpretation.

457
458 *4.2 Structure maps*

459 TWT horizon maps were constructed from the interpreted horizons to illustrate the interpreted
460 3D structure (Fig. 9).

461 The basement consists of highly deformed, metamorphosed Caledonian schists and
462 gneisses. The Top Basement geometry, equivalent to the base of the sedimentary basin fill,
463 is dominated by a 10-20 km wide E-W trending asymmetric depression on the downthrown
464 northern side of the Stublick fault: this is the Northumberland Trough (Fig. 9A). The trace of
465 the Stublick Fault is not straight and shows a prominent 'embayment' just east of the centre.
466 The TWT to the Top Basement along the fault commonly exceeds 2 s, with major structural
467 lows on both sides of the embayment and another two minor lows interpreted within the
468 embayment itself. We interpret that the Stublick Fault formed through linkage of several
469 smaller faults, probably through relay ramp breaching. At Top Basement level the easternmost
470 part of the Stublick Fault seems to have initiated as a NE-SE striking, basin boundary-parallel
471 fault before linking up with the more E-W striking segments of the Stublick Fault.. The
472 maximum displacements of each of these smaller faults are still recognisable as local TWT
473 lows along the fault strike.

474 The Ninety-Fathom Fault can only be reliably interpreted using Top Basement. The
475 interpreted segment is of a limited extent but it too shows a non-linear geometry with highly
476 variable strikes. The Top Basement deepens towards the east along this fault, forming a relay
477 ramp between the Stublick fault and the Ninety-Fathom fault. A basement high belonging to
478 the Alston Block is interpreted in the SE of the area, in the foot-wall of the Ninety Fathom Fault.

479 The Top Basement along the northern margin of the trough is characterised by a southerly
480 dip and the absence of a continuous fault zone. The northern margin is around ~1.5 s TWT to
481 basement, but rapidly increases towards the trough centre before levelling out somewhat. The
482 Antonstown Fault and the Sweethope Fault cut through the Top Basement near the steeper

1063
1064
1065
1066
1067
1068
1069
1070
1071
1072
1073
1074
1075
1076
1077
1078
1079
1080
1081
1082
1083
1084
1085
1086
1087
1088
1089
1090
1091
1092
1093
1094
1095
1096
1097
1098
1099
1100
1101
1102
1103
1104
1105
1106
1107
1108
1109
1110
1111
1112
1113
1114
1115
1116
1117
1118
1119
1120
1121

483 dips, and sub-seismic resolution faults may be present along the zone of steeper dips (with
484 associated relay ramps contributing to the basement topography in this region), but overall the
485 northern margin does not show obvious faulting within the basement at seismic resolution.
486 The maximum throw on both the Antonstown Fault and the Sweethope Fault at basement
487 level is around 0.25 s TWT (~300-500 m). Towards the east, the Top Basement becomes
488 east-dipping.

489 The Top Fell Sandstone is significantly more faulted than the Top Basement, especially
490 along the northern margin of the basement trough (Fig. 9B). The dominant strike of the faults
491 is E-W to ENE-WSW, although ESE-WNW striking faults also occur in the east. North-dipping
492 faults are more frequent than south-dipping faults. The throw on most faults is too small to
493 have much impact at the scale of the structure map. The most significant faults are the
494 Antonstown Fault and the Sweethope Fault, although the maximum throw at this level is
495 reduced to 0.10 s and 0.20 s TWT respectively. However, the strike lengths of both faults have
496 significantly increased relative to what can be interpreted from the seismic at Top Basement
497 level, especially that of the Sweethope Fault. In addition, the distance between the faults and,
498 consequently, the width of the minor graben between them has also increased. Other
499 significant faults within this zone include the Causey Park Fault, the Hallington Reservoir Fault,
500 and both Stobswood Faults. The maximum throw on these faults does not exceed 0.08 s TWT
501 but they have significant lengths of up to several tens of kilometres. Several relay ramps can
502 be identified between the various faults.

503 The elongated depression in the Stublick Fault hanging-wall is significantly narrower than
504 the depression defined by the Top Basement. The eastward projection of the Stublick Fault
505 potentially links with the up-dip continuation of the Ninety-Fathom Fault, although this cannot
506 be determined from the available data. Structural lows along the Stublick Fault are confined
507 to the eastern part of the study area, whilst towards the west the lows are situated near smaller
508 (splay?) faults.

509 The Fell Sandstone Formation reaches outcrop in the western of the area of the interpreted
510 seismic lines. The eastern part of the structure map is again dominated by a shallow eastward

1122
1123
1124 511 dip, reflecting the arcuate outcrop pattern of the Carboniferous sediments as they become
1125
1126 512 east-dipping (Fig. 4).

1128 513 The Top Tyne Limestone Formation and the Top Alston Formation cover a smaller area in
1129
1130 514 the interpretation as erosion has removed them from the NW (Figs. 9C and 9D). The general
1131
1132 515 structure of both horizons is very similar to the Top Fell Sandstone Formation in terms of dip
1133
1134 516 trends and faulting. The horizons dip generally southwards towards the Stublick Fault, forming
1135
1136 517 small trough structures, with a gentle easterly dip becoming dominant towards the east part of
1137
1138 518 the map. The syncline near the western part of the Stublick Fault is present in the Top Tyne
1139
1140 519 Limestone Formation map but can no longer be identified in the younger Alston Formation.
1141
1142 520 Farther north, the Sweethope Fault, the Causey Park Fault, the Stobswood Fault and the
1143
1144 521 Hallington Reservoir Fault, along with several minor faults, are all interpreted to penetrate up
1145
1146 522 to the Top Alston Formation. Note, however, that the seismic data are not processed above
1147
1148 523 ~0.2 s TWT, and that here the horizons have been interpreted by extrapolation from deeper
1149
1150 524 reflectors, introducing uncertainty into the near-surface fault identification, even compared with
1151
1152 525 outcrop data. Either way, it is clear that the majority of the faults have been active after (and
1153
1154 526 possibly during) the deposition of these Viséan packages although the displacements are
1155
1156 527 generally small (~200 m at most).

1157 528 1158 1159 529 *4.3 Thickness maps*

1160
1161 530 3D maps illustrating thickness variations within each interpreted package (i.e. TWT thickness
1162
1163 531 maps) can be constructed by subtracting the thicknesses of the overlying packages from the
1164
1165 532 TWT depth to the base of the package in question (Fig. 1D). The TWT thickness maps for the
1166
1167 533 interpreted packages are shown in Fig. 10. Figure 10A illustrates the thickening of the Lower
1168
1169 534 Groups (Top Basement to Top Fell Sandstone) from the minimum value of around 0.63 s TWT
1170
1171 535 in the NE part of the study area, to a maximum of 2.00 s TWT in the W. This represents a 52%
1172
1173 536 deviation from the average thickness (min thickness + max thickness / 2) of 1.32 s TWT for
1174
1175 537 this package. The maximum thickness occurs approximately 5 km north of the Stublick Fault
1176
1177 538 and increases westwards along the Northumberland Trough; this is probably due to the

1181
1182
1183 539 sediment accumulation pattern switching from thickening towards the fault during Courceyan-
1184
1185 540 Chadian active faulting, to thickening away from the fault after active rifting waned during the
1186
1187 541 subsequent sag phase. Although the Stublick Fault has the most noticeable effect on the
1188
1189 542 thickness distribution, the Antonstown-Sweethope Fault zone also seem to have a minor
1190
1191 543 control the thickening on the northern margin of the trough, indicating that they may have been
1192
1193 544 active during the earliest Carboniferous.

1195 545 The Tyne Limestone Formation (Top Fell Sandstone to Top Tyne Limestone) has a
1196
1197 546 minimum thickness of 0.21 s TWT and a maximum thickness of 0.52 s TWT (Fig. 10B). The
1198
1199 547 thickest interval is found in the central part with a 42% change from the average sequence
1200
1201 548 thickness of 0.37 s TWT. The maximum thickness is attained farther east than in the Lower
1202
1203 549 Groups and around 10-12 km to the north of the Stublick Fault, centred between two smaller,
1204
1205 550 unnamed faults between the Stublick Fault and the Sweethope Fault. This thickness change
1206
1207 551 does not seem to be controlled by any earlier (basement) faults. The thickness change is close
1208
1209 552 to the approximate interpretational error margin of ~0.05 s TWT, but another possible
1210
1211 553 explanation is that there was some active normal faulting along the two unnamed faults and/or
1212
1213 554 differential compaction during the sag phase during the Asbian when these sediments were
1214
1215 555 deposited. Another area with larger than average thicknesses is present westwards along the
1216
1217 556 trough, with thicknesses commonly at ~0.5 s TWT, changing rapidly from ~0.3-0.4 s TWT and
1218
1219 557 therefore not within interpretational error margin. Sub-resolution Asbian faulting may control
1220
1221 558 this thickening; alternatively some local accommodation space for the Asbian sediments may
1222
1223 559 have remained from the earlier basin subsidence and differential sediment compaction.

1224 560 The Alston Formation (Top Tyne Limestone to Top Alston) thickness map is of limited use
1225
1226 561 due to its small extent before this formation reaches outcrop (Fig. 10C). Overall, the Alston
1227
1228 562 Formation thickens slightly southwards towards the Stublick Fault, from around 0.12 s TWT in
1229
1230 563 the north to a maximum of 0.24 s TWT 2-3 km north of the fault. This is a 33% change from a
1231
1232 564 0.18 s TWT average thickness. However, most of the thickness variation seen in this package
1233
1234 565 is within the interpretational error margin of ~0.05 s TWT. The trend towards greater
1235
1236
1237
1238
1239

1240
1241
1242
1243
1244
1245
1246
1247
1248
1249
1250
1251
1252
1253
1254
1255
1256
1257
1258
1259
1260
1261
1262
1263
1264
1265
1266
1267
1268
1269
1270
1271
1272
1273
1274
1275
1276
1277
1278
1279
1280
1281
1282
1283
1284
1285
1286
1287
1288
1289
1290
1291
1292
1293
1294
1295
1296
1297
1298

566 thicknesses towards the SW of the map is very poorly constrained by the seismic data, and
567 noisy seismic inhibits reliable interpretation of Top Alston Fm. in the SW.

568

569 **5. Discussion**

570 There is a clear overall reduction in magnitude of thickness variation upwards within the
571 sedimentary succession, reflecting the transition from syn-rift to late- or post-rift packages.
572 The older, deeper packages, especially within the middle and lower Lower Groups, display
573 much greater thickness variations with thickness increases both towards the Stublick Fault
574 and towards the deeper parts of the basin, both in terms of absolute values and relative to the
575 average thickness of each package. The higher Lower Groups and the Tyne Limestone
576 Formation seem to have been affected by the waning fault activity along the original, basin-
577 bounding faults and by the onset of the thermal sag phase with thickening increasingly towards
578 the basin centre; this overall subsidence is reflected in the increasingly marine (limestone)
579 successions of the ~Chadian to Asbian packages. The observations described above, made
580 from the interpreted 3D maps therefore help us to constrain the fault timings, relative fault
581 displacement magnitudes, and the distribution and geometries of the syn-rift packages.

582 To summarize, the Northumberland Trough is controlled by the large east-west trending,
583 north-dipping Stublick Fault. The kilometre-scale throw affecting the basement is consistent
584 with the Stublick fault being a part of the basin-bounding fault system that comprises the
585 Ninety-Fathom Fault, Stublick Fault and the Maryport Fault systems (Fig. 2 inset). The Stublick
586 Fault system is, except for its south-easternmost part, approximately E-W trending as opposed
587 to the other two which have generally more NE-SW orientations; this may indicate that Stublick
588 Fault formed a large breaching fault system within a relay ramp between the Ninety-Fathom
589 Fault and the Maryport Fault systems. The seismic data does not extend far enough west,
590 however, to draw definite conclusions about this. In more detail, the discrete structural low
591 points seen in Fig. 9 in the hanging-wall of the Stublick fault at Top basement level may
592 represent individual depocentres, hinting at a possible segmentation of the Stublick fault (i.e.
593 lateral fault linkage during fault growth; Cowie et al., 2000). This interpretation is also

1299
1300
1301
1302
1303
1304
1305
1306
1307
1308
1309
1310
1311
1312
1313
1314
1315
1316
1317
1318
1319
1320
1321
1322
1323
1324
1325
1326
1327
1328
1329
1330
1331
1332
1333
1334
1335
1336
1337
1338
1339
1340
1341
1342
1343
1344
1345
1346
1347
1348
1349
1350
1351
1352
1353
1354
1355
1356
1357

594 supported by the non-linear nature of the fault with the strike changes correlating with the
595 structural lows. The Ninety Fathom fault in the far SE of the area runs parallel to the NE
596 segments of the Stublick fault and also displays kilometre-scale throw at the Top Basement
597 level. It is therefore probably the en-echelon, right-stepping, eastwards continuation of the
598 basin-bounding fault system in this area. The Stublick and Ninety Fathom faults are interpreted
599 to be soft-linked at Top Basement level, separated by an east-dipping relay ramp, although
600 this is poorly constrained and the relay ramp between the two faults may be breached (Figure
601 10A).

602 Other significant, early rift-related faults are the Sweethope Fault and the Antonstown Fault.
603 Based on the interpreted variability of throw and strike of these (and many other) faults, they
604 too seem to have been highly segmented initially and gained length through relay ramp
605 breakage.

606 Although we were unable to interpret horizons older than the Top Fell Sandstone
607 Formation, an attempt was made to further constrain the initiation of rifting. The Early
608 Carboniferous, syn-rift Lower Groups thicken into the Stublick Fault hanging-wall (Figs. 8A,
609 10A). The thickening is especially visible in the middle and lower parts of the Lower Groups,
610 indicating that Stublick Fault was active when this part of the succession was deposited, i.e.
611 during the Early Carboniferous (~Courceyan-Chadian). On dip lines (Fig. 8A) the thickening
612 within the Lower Groups switches approximately in the middle of the succession to thicken
613 away from the Stublick Fault, possibly indicating the waning of active faulting in this area and
614 initiation of the thermal subsidence (sag) phase. Both the top and the bottom ~0.3 s of the
615 group maintain an approximately constant thickness. This suggests that a pre-rift package
616 may present above the basement, and a syn-rift succession is correspondingly present
617 towards the top of the package. The reflections just above the basement have previously been
618 interpreted as basaltic lavas associated with the onset of rifting (Leeder, 1974; Fraser and
619 Gawthorpe, 2003). We consider that interpreting this interval as pre-rift sediments rather than
620 basalts is more consistent with the >40km-scale extent, the modest acoustic impedance
621 contrast, and the regular geometry of this package.

1358
1359
1360
1361
1362
1363
1364
1365
1366
1367
1368
1369
1370
1371
1372
1373
1374
1375
1376
1377
1378
1379
1380
1381
1382
1383
1384
1385
1386
1387
1388
1389
1390
1391
1392
1393
1394
1395
1396
1397
1398
1399
1400
1401
1402
1403
1404
1405
1406
1407
1408
1409
1410
1411
1412
1413
1414
1415
1416

622 The growth strata thickening is more obvious on strike lines (Fig. 8B) than on dip lines.
623 Westwards thickening of the Lower Groups parallel to the Stublick fault is interpreted to be
624 caused by the general deepening of the basin towards the west in addition to the faulting and
625 sag phases, controlled in this area mainly by the Stublick Fault system but also the
626 Antonstown-Sweethope fault system.

627 Both the Tyne Limestone Formation and the Alston Formation are extensively faulted, with
628 especially the Tyne Formation showing some possible thickness variation related to the two
629 unnamed faults in the centre of the thickness map (Fig. 10B). Whilst it is possible that minor
630 faulting continued into (or initiated during) the Asbian-Brigantian, some of the thickness
631 variation may be explained by differential compaction during the sag phase. The data does
632 not allow determining with certainty whether these minor faults nucleated on or reactivated
633 existing Lower Carboniferous rift-related faults within the Lower Groups, but this seems
634 unlikely given that the faults do not seem to affect the basement. This makes them unlikely to
635 be important for any possible Irish-style mineralisation in this area as the Irish-style
636 mineralisation is linked with major faults penetrating the basement.

637 The interpretation of the study area is predominantly consistent with the accepted
638 geological history and existing interpretations of Northumberland Trough (e.g. Collier, 1989;
639 Chadwick et al., 1995; Stone et al., 2010). Rifting occurred under approximately north-south
640 orientated extension during the Lower Carboniferous, with the majority of deformation
641 localising into ~NE-SW trending controlled the older Caledonian basement fabrics; the slightly
642 oblique ~E-W normal fault systems such as the Stublick Fault possibly formed as relay-ramp
643 breaching structures between the NE-SW right-stepping faults. The prediction arising from this
644 is that if the overall extension was NE-SW orientated, the E-W trending faults are probably
645 dextral-normal faults, whilst the NE-SW trending faults are dominantly dip-slip faults. If this is
646 the case, the transtensional nature of the E-W faults could be expected to enhance fluid flow
647 into these fault zones. Either way, the basin analysis approach illustrated here provides closer
648 insights into the timing and the internal geometries of the faults, the fault linkage histories, and

1417
1418
1419
1420
1421
1422
1423
1424
1425
1426
1427
1428
1429
1430
1431
1432
1433
1434
1435
1436
1437
1438
1439
1440
1441
1442
1443
1444
1445
1446
1447
1448
1449
1450
1451
1452
1453
1454
1455
1456
1457
1458
1459
1460
1461
1462
1463
1464
1465
1466
1467
1468
1469
1470
1471
1472
1473
1474
1475

649 the geometries of the coeval depositional packages, understanding of which is key for
650 exploration of basin ores.

651
652 *5.1. Comparison with Ireland and assessment of mineralisation potential*

653 From the observations made in the previous sections, and with the corresponding timings
654 and geometries in the Pb-Zn play of Ireland well known, we can now perform a more robust
655 comparison between Ireland and Northumberland. The scale and the timing of the Early
656 Carboniferous faulting corresponds exactly to the scale and activity of the major fault systems
657 controlling the Irish Pb-Zn mineralisation (e.g. Ashton et al., 2015, 2018). In Ireland, the main
658 faults that control the formation and location of Pb-Zn deposits are of Courcayan-Arundian
659 age, although another possible regional rifting event is identified during Asbian-Brigantian (e.g.
660 Fraser and Gawthorpe, 1990). E-W or ENE-WSW trending syn-sedimentary normal faults with
661 displacements of hundreds of metres and possibly up to 1.5-2 km within the basement (Table
662 2; e.g. Hitzman and Beaty, 1996; Ashton et al., 2018). Deposits are normally associated with
663 fault arrays rather than isolated faults, with fluid feeder points typically occurring at areas of
664 maximum fault throw and in broken relay ramps (Hitzman, 1999; Torremans et al., 2018). The
665 crucial role of breached/highly fractured relay ramps at various scales as fluid flow focal points
666 has been suggested at least at Silvermines and Lisheen (Torremans et al., 2018; Kyne et al.,
667 2019) but the Navan deposit and its satellite Tara Deep also show complex fault-ore-breached
668 relay ramp relationships at various scales (see e.g. Fig. 10 in Ashton et al., 2018).

669 The first-order requirement for faulting extending to the basement, probably Courcayan-
670 Arundian in age, and with throw of at least ~200 m (Table 2) is satisfied by many major faults
671 in Northumberland, but excludes most of the other, isolated faults identified within the study
672 area as they do not affect the basement and have small throws. The major Stublick-Ninety
673 Fathom fault system, along with the Antonstown- Sweethope Fault zone have a suitable
674 Courcayan-Arundian age; possibly also the Stobswood Fault, Causey Park Fault and
675 Hallington Reservoir Fault (Table 2). Significant throws and relay ramp breakage, similar to
676 the Irish faults, is evident along the Stublick Fault (Fig. 9A). The Stublick Fault zone itself may

1476
1477
1478
1479
1480
1481
1482
1483
1484
1485
1486
1487
1488
1489
1490
1491
1492
1493
1494
1495
1496
1497
1498
1499
1500
1501
1502
1503
1504
1505
1506
1507
1508
1509
1510
1511
1512
1513
1514
1515
1516
1517
1518
1519
1520
1521
1522
1523
1524
1525
1526
1527
1528
1529
1530
1531
1532
1533
1534

677 in its eastern parts be a regional-scale relay ramp-breaching fault linking the more NE-SW
678 trending Maryport Fault and Ninety-Fathom Fault systems (Fig. 2, inset), although the seismic
679 data coverage is insufficient to determine this with any certainty. If Irish-type mineralisation
680 exists in the Northumberland Trough, its fluid feeder channels are similarly to Ireland most
681 likely related to the points of maximum throw or, more likely, to the (breached) relay ramps
682 identified in along the central and western parts of the Stublick Fault in Fig. 9A. The larger
683 relay ramp between the Stublick Fault and the Ninety-Fathom Fault (Fig. 9A) is less likely to
684 control mineralisation because i) the basin shallows significantly to the east and, crucially, the
685 relay ramp formed within a structural high with non-deposition of Early Carboniferous
686 carbonates; and ii) it does not seem to be breached at basement level, although the data
687 quality in the area of this relay ramp may prevent detection of any breaching faults.

688 The potential for the faults within the Northumberland Trough to act as mineralising fluid
689 conduits is shown by baryte and lead mineralisation on the Stublick Fault itself (Dunham,
690 1990). The Lower Carboniferous sequences are not exposed in this area, but exposures are
691 found 10-20 km north and northwest with some stratabound base metal mineralisation in the
692 proximity of other, southeast-dipping normal faults (near Langholm and Saughtree; Fig. 2;
693 Gallagher et al., 1977; Smith et al., 1996). The timing and downward extents of the faults near
694 Langholm and Saughtree remains unresolved as the seismic data do not extend this far north.

695 Based on the interpreted structural evolution and the tectonic history of the area, we
696 propose a refined structural model for the Carboniferous evolution of the Northumberland
697 Trough and how it may be linked to Irish-style mineralisation at depth (Fig. 11A-C).

698 Another key requirement for Irish-style mineralization is the presence of carbonate
699 packages into which the mineralizing fluids can penetrate. The characteristics of the thick syn-
700 rift Lower Groups within the sub-surface Northumberland Trough remain mostly unknown,
701 although the outcropping part of this sequence in the eastern part of the study area shows
702 contrasting fluvial input from the NE and marine input from the SW (Johnson 1980; Leeder et
703 al. 1989). Later Carboniferous (Asbian to Pendeleian) clastic-carbonate cycles of up to 50 m
704 thickness, with the marine limestone component within each cycle of up to 30 m thickness,

1535
1536
1537 705 have been logged in the broader area of NE England (Gallagher et al., 1977; Smith et al.,
1538
1539 706 1996; Tucker et al. 2003; Dean et al. 2011). As such, whilst this paper has highlighted the
1540
1541 707 potential from the structural geology viewpoint for Early Carboniferous mineralisation within
1542
1543 708 the Northumberland Trough, the presence of suitable host lithologies at depth remains to be
1544
1545 709 tested through drilling. The presence of outcropping thin marine limestones, the thicknesses
1546
1547 710 of which seem to increase towards the west and include Lower Carboniferous sulphide-
1548
1549 711 mineralized horizons (Gallagher et al., 1977; Smith et al., 1996) is however an encouraging
1550
1551 712 starting point.

1552
1553 713 The depth to the target horizon for any potential Irish-type mineralisation within the
1554
1555 714 Northumberland Trough will probably be defined by the lowest carbonate sequences within
1556
1557 715 the syn-rift Lower Groups, adjacent to suitable feeder faults, although in Ireland the ore is not
1558
1559 716 always in the lowermost carbonate sequence (e.g. Torremans et al., 2018). Such a horizon
1560
1561 717 could lie anywhere between the Top Basement and the Top Fell Sandstone reflectors.
1562
1563 718 However, we consider that it is most likely to be present within the middle or towards the top
1564
1565 719 of the Lower Groups once the basin had subsided enough to be influenced by significant
1566
1567 720 marine input: the most prominently wedge-shaped packages with thickening towards the main
1568
1569 721 faults, marking the most active rifting period, are seen in the lower and middle parts of the
1570
1571 722 Lower Groups package (Fig. 8). As identified in this study, the most prospective feeder faults
1572
1573 723 within Northumberland are the Sweethope and Stublick faults. Around the intrabasinal
1574
1575 724 Sweethope fault, the Top Fell Sandstone is typically located at 0.2-0.6 s TWT (~400-1200 m
1576
1577 725 with 4000 m s⁻¹), whereas adjacent to the Stublick fault the top Fell Sandstone usually exceeds
1578
1579 726 0.6 s TWT (>1200 m).

1580 727 1581 1582 728 *5.2. Possible link to the Permian mineralisation of the North Pennine Orefield*

1583
1584 729 The cause of the Permian mineralising event is debated as, despite some evidence of
1585
1586 730 regional extension, subsidence and high heat flow at the time, there was no major foreland
1587
1588 731 basin/rifting which would be typical for most MVT ores (e.g. Collier, 1989). The Weardale
1589
1590 732 Granite, a concealed Devonian age batholith (Dunham et al., 1961), probably controlled much

1594
1595
1596 733 of the mineralizing fluid flow in the Alston Block on account of higher fracture density and
1597
1598 734 connectivity (Bott & Mason-Smith 1957; Kimbell et al. 2010), but the fluid and metal sources
1599
1600 735 remain enigmatic. The NPO mineralisation has been suggested to represent a fluoritic sub-
1601
1602 736 type MVT ore, the fluid sources being mixed but probably mostly originating from the adjacent
1603
1604 737 basins (e.g. Crowley et al. 1997; Cann and Banks, 2001; Baba et al., 2019; Kraemer et al.
1605
1606 738 2019). The MVT model for the NPO envisages dewatering of basin facies sediments (those
1607
1608 739 in the Northumberland and Stainmore Troughs) to generate carrier fluids. Most of the 'MVT-
1609
1610 740 style' models agree that the basinal fluids migrate laterally into the Weardale granite 'plumbing
1611
1612 741 system', before mixing with other fluids and travelling upwards along fractures in the granite
1613
1614 742 into the Upper Carboniferous rocks on the Alston Block, where they cool and deposit minerals
1615
1616 743 (Fig. 7; Jackson and Beales, 1967; Dunham, 1983; Brown et al., 1987; Bott and Smith, 2018).

1617
1618 744 The metal sources for the known Permian mineralisation of the NPO are unknown and
1619
1620 745 various sources from underplated mafic magmas to leaching of the Weardale granite have
1621
1622 746 been suggested. Cann and Banks (2001) use sulphur isotopes to infer the lead probably
1623
1624 747 originated from basement, but the evidence is inconclusive especially as the sulphates may
1625
1626 748 be associated with the surface brines (Bouch et al., 2006). Dempsey (2016), on the other
1627
1628 749 hand, found that at least some of the osmium in NPO pyrites originated from the mantle (i.e.
1629
1630 750 underplated mafic magma potentially underlying the Alston Block), although there was also a
1631
1632 751 significant sample group of higher osmium isotope ratios indicating other, unknown source(s).
1633
1634 752 Kraemer et al. (2019) argue against mafic rocks as a source of fluids and metals, inferring that
1635
1636 753 the REY patterns within the veins correspond better to leaching of metals from basinal shales
1637
1638 754 or the Weardale granite.

1639 755 Based on the published literature, an intrabasinal metal source from an Early Carboniferous
1640
1641 756 lead-zinc base metal deposit cannot, therefore, be ruled out. There is a significant body of
1642
1643 757 evidence that most of the fluid originated from the basins adjacent to the Alston Block,
1644
1645 758 although mixing with both surface and magmatic fluids is possible (e.g. Jackson and Beales,
1646
1647 759 1967; Dunham, 1983; Cann and Banks, 2001; Bott and Smith, 2018). Whilst the fluids and the
1648
1649 760 metals do not need to originate from the same source, we hypothesise that the easiest

1653
1654
1655
1656
1657
1658
1659
1660
1661
1662
1663
1664
1665
1666
1667
1668
1669
1670
1671
1672
1673
1674
1675
1676
1677
1678
1679
1680
1681
1682
1683
1684
1685
1686
1687
1688
1689
1690
1691
1692
1693
1694
1695
1696
1697
1698
1699
1700
1701
1702
1703
1704
1705
1706
1707
1708
1709
1710
1711

761 explanation for the presence of the Permian mineralization is the remobilisation of older
762 mineralisation at depth within the basins adjacent to the NPO structural highs (Fig. 11D).
763 Hydrothermal fluid-assisted remobilisation of lead and zinc from galena and sphalerite is a
764 globally known phenomenon and has been reported from e.g. the Ramsbeck Pb-Zn deposit
765 in Germany (Wagner and Boyce, 2001). The basement signature of Cann and Banks (2001)
766 is not inconsistent with a remobilisation hypothesis as any Irish-type ores at depth are likely to
767 carry a basement isotope signature which can be inherited in subsequent remobilisation. The
768 low concentrations of lead (galena) in the sphalerite-dominated Permian NPO deposits are
769 consistent with the remobilisation hypothesis: e.g. Barrett and Anderson (1988) show that ZnS
770 is more soluble than PbS by a factor of up to 100 in NaCl brines of up to 300°C.

771 Our remobilisation hypothesis is also consistent with the 'circulation cell' model proposed
772 by e.g. Bott & Smith (2018) but refines it by suggesting that not only fluids but also most if not
773 all of the metals originated from remobilized ores within the Northumberland Trough and/or
774 other basins adjacent to the NPO. The presence of at least one Carboniferous sealing horizon
775 such as shale or evaporite within the Northumberland Trough would help to constrain fluid
776 flow. Evidence for the presence of such horizons is given by e.g. Day (1970) and Johnson
777 (1980) who report marine shales and evaporite layers within the Border Group in the
778 northwestern part of the Northumberland Trough.

779

780 **6. Conclusions**

781 We have used basin analysis through structural interpretation of seismic reflection data to
782 investigate the potential for syn-rift base metal deposition in the Northumberland Trough. Syn-
783 sedimentary faulting in the Northumberland Trough associated with active rifting occurred from
784 the earliest Carboniferous through to at least the late Viséan, subsequently giving way to
785 regional subsidence and, during the Permian, to renewed faulting. ENE trending arrays of
786 basin-bounding and intrabasinal normal faults are studied in detail in this paper, in terms of
787 their geometries and timings and their associated sedimentary growth packages. The
788 interpreted scales and the Early Carboniferous timing of the faulting and the sedimentation in

1712
1713
1714
1715
1716
1717
1718
1719
1720
1721
1722
1723
1724
1725
1726
1727
1728
1729
1730
1731
1732
1733
1734
1735
1736
1737
1738
1739
1740
1741
1742
1743
1744
1745
1746
1747
1748
1749
1750
1751
1752
1753
1754
1755
1756
1757
1758
1759
1760
1761
1762
1763
1764
1765
1766
1767
1768
1769
1770

789 the study area is comparable with the fault and sedimentation system that controls lead-zinc
790 mineralisation in the Irish Midlands: this opens up the possibility that the Irish Pb-Zn play
791 extends into northern England. We suggest a refined model for the evolution of the
792 Northumberland Trough, similar to the Irish stratabound Pb-Zn deposits. We suggest that the
793 faults grew through hard linkage by breaching of relay ramps, possibly associated with flow of
794 mineralising fluids from the basement, and identify potential locations for such mineralisation.
795 The presence of suitable host Early Carboniferous host lithologies and stratabound base metal
796 mineralisation at depth remains to be tested by drilling. If present, it could offer the simplest
797 explanation for the presence of the known Permian mineralised veins in the North Pennines
798 Orefield (NPO): through (partial) remobilisation of Early Carboniferous base metal ores within
799 the adjacent basin(s).

800 Our study demonstrates that basin analysis using seismic reflection interpretation is a
801 powerful tool in basin ore exploration. It allows a much more detailed insight into the timing,
802 geometry and extent of faulting along with the extent of and thickness variations within the
803 syn-rift sedimentary packages than is possible through surface observations and sampling
804 alone. Crucially, it also allows identification of zones of structural complexity such as
805 (breached) relay ramps which commonly function as channels for mineralising basement
806 fluids. Establishing the relationships of these fundamental mineralisation-controlling features
807 is a crucial step in a basin ore play analysis. As shown in this paper, a detailed consideration
808 of the timing, geometry and linkage of the faulting with respect to the sedimentation allows
809 both assessing the general potential of base metal mineralisation and a more precise
810 identification of potentially suitable areas for further investigation.

811
812 **Acknowledgements**

813 This work is based on the MSc thesis by AJ in Structural Geology with Geophysics at the
814 University of Leeds under a scholarship from BP plc. Sincere thanks to the UK Onshore
815 Geophysical Library (UKOGL) for providing the data for this work. Images of all of the UK
816 onshore seismic lines, including those used in this study, and some offshore lines can be

1771
1772
1773 817 viewed with their interactive viewer at www.ukoggl.org. We are also grateful to the Editor-in-
1774
1775 818 Chief Franco Pirajno and for the constructive and helpful reviews of George Gibson and Koen
1776
1777 819 Torremans.
1778
1779 820
1780
1781
1782
1783
1784
1785
1786
1787
1788
1789
1790
1791
1792
1793
1794
1795
1796
1797
1798
1799
1800
1801
1802
1803
1804
1805
1806
1807
1808
1809
1810
1811
1812
1813
1814
1815
1816
1817
1818
1819
1820
1821
1822
1823
1824
1825
1826
1827
1828
1829

1830
1831
1832 **821 Figure captions**
1833
1834 **822**

1835 **823 Fig. 1.** Schematic illustrations of the relationships between sediment deposition and faulting,
1836 and of the seismic interpretation method and main outputs. Critically, if the age of the syn-
1837 824 rift sediments is known, the timing of the faulting can be established. A) Configuration of
1838 825 the basement and overlying sediments before faulting; B) During active faulting, the
1839 826 sediments will be preferentially deposit into the wedge-shaped accommodation space in
1840 827 the hanging-wall created by the faulting. This wedge geometry with thickening of the
1841 828 sedimentary package towards the active fault is very typical and diagnostic of syn-rift
1842 829 sediments; C) After the fault activity ceases, post-fault sediment deposition will blanket the
1843 830 area with relatively little thickness variation, although some thickening can occur in areas
1844 831 where the basin was not completely filled during active faulting; D) Typical 2D seismic
1845 832 interpretation approach to basin analysis. A grid of seismic reflection profiles is interpreted
1846 833 for structures (e.g. faults) and depths of formation boundaries. Any borehole (well) data or
1847 834 exposure at outcrop will greatly help in constraining the boundaries at depth. The
1848 835 interpretations in the 2D grid are then interpolated to '3D' (2.5D) interpretations, i.e.
1849 836 structural (depth/isochron) and thickness maps which can be used for further interpretation
1850 837 of the basin evolution. A thickness map for an interval of interest is constructed by
1851 838 subtracting the thicknesses of the overlying packages (X) from the thickness of the entire
1852 839 succession (X+Y) along the entire length of the interpreted lines; e.g. (X+Y)-X in the location
1853 840 shown along Line 1 in this figure.
1854 841
1855 842
1856 843

1857 844 **Fig. 2.** Generalized regional map showing the main Caledonian to Carboniferous tectonic
1858 845 elements of Ireland and Northern England-Southern Scotland, along with three mined Irish-
1859 846 type deposits in Ireland. Carboniferous normal faults: SF, Stublick fault; NFF, Ninety-
1860 847 Fathom Fault; SCF, South Craven Fault; MCF, Mid-Craven Fault; PF, Pendle Fault; NF,
1861 848 Navan Fault; SMF, Silvermines Fault. Irish-type Pb-Zn deposits: N, Navan deposit; T,
1862 849 Tynagh deposit; S, Silvermines and Lisheen deposits. Modified from Jones et al. (1994)
1863 850 and Treagus (1992). Inset: Map of the main sub-surface Carboniferous tectonic elements
1864 851 in the Northern Pennines Orefield and Solway-Northumberland Basin areas as interpreted
1865 852 by Chadwick et al. (1995). The area of our study shown in Fig. 3. is indicated with a
1866 853 rectangle.
1867 854
1868 855
1869 856
1870 857
1871 858
1872 859
1873 860
1874 861
1875 862
1876 863
1877 864
1878 865
1879 866
1880 867
1881 868
1882 869
1883 870
1884 871
1885 872
1886 873
1887 874
1888 875

1886 876 **Fig. 3.** Generalized map of the surface geology of the Alston block and southern
1887 877 Northumberland Trough, including known occurrences of Permian vein-style Pb-Zn
1888 878 mineralisation. Modified from Stone et al. (2010) and Kimbell et al. (2010).
1889 879
1890 880
1891 881
1892 882
1893 883
1894 884
1895 885
1896 886
1897 887
1898 888

1889
1890
1891
1892
1893
1894
1895
1896
1897
1898
1899
1900
1901
1902
1903
1904
1905
1906
1907
1908
1909
1910
1911
1912
1913
1914
1915
1916
1917
1918
1919
1920
1921
1922
1923
1924
1925
1926
1927
1928
1929
1930
1931
1932
1933
1934
1935
1936
1937
1938
1939
1940
1941
1942
1943
1944
1945
1946
1947

858 **Fig. 4.** Generalized geological map of the study area with the seismic reflection profiles. The
859 type sections in Figures 7A and 7B are indicated with the stippled red lines.

860
861 **Fig. 5.** Generalized stratigraphic column for the Northumberland Trough and Alston Block.

862
863 **Fig 6.** Schematic illustration for the formation of Irish-type Pb-Zn deposits. They form in
864 shallow marine carbonate shelves by stratabound replacement into calcareous host rocks.
865 Mixing of sulphur-rich seawater/brines and metal-bearing hot basement fluids is typically
866 postulated (e.g. Ashton et al. 2015).

867
868 **Fig 7.** Schematic model for the fluid system within the NPO (modified from Bott and Smith,
869 2018). According to the model, the highly fractured and permeable Weardale granite hosted
870 a convection cell which drew in saline fluids from adjacent deep Carboniferous troughs.
871 The model postulates that the heat to drive the convection cells may have originated from
872 underplated magmas, although others have suggested that the high heat flow and fractured
873 nature of the granite will be enough to drive the cell (e.g. Brown et al., 1987). The pictured
874 Bott and Smith (2018) model suggests that the metals were derived from the mafic
875 magmas; other models for metal source suggest leaching from basin sediments and/or the
876 Weardale granite itself (e.g. Crowley et al. 1997). See section 5.2 for full discussion.

877
878 **Fig 8.** Interpreted seismic type sections, showing the general sequence architecture and main
879 faults using higher quality lines. The line locations are highlighted in Fig. 4. Formation
880 boundaries are shown by coloured solid lines; dashed red lines within the Lower Groups
881 are delineating possible pre- and post-rift packages; also additional, arbitrary horizons are
882 shown to demonstrate the within-sequence wedge geometry of this package, typical for
883 syn-faulting growth packages (i.e. thinning towards the north and the east, especially in the
884 middle and lower parts of the Lower Groups). (a) Seismic line TOC86-V102 which runs
885 approximately north-south. (b) Seismic line TOC87-V112 which runs roughly west-east.
886 This figure also shows an example of how mis-ties were mitigated: the basement in (a)
887 appears higher than in (b) so that the horizons in (a) had to be manually adjusted
888 downwards; note that manually lowering the horizon in (a) matched the outcropping
889 formation boundaries.

890
891 **Fig 9.** 3D isochron maps of the interpreted formation boundaries (i.e. seismic surface structure
892 maps), interpolated from the 2D seismic line interpretations (in TWT: 1 s equals
893 approximately 1.5-2 km depending on the lithology). Major normal faults (tick-marks on
894 hanging-wall) are numbered with corresponding names at the base of the figures. Grey

1948
1949
1950
1951
1952
1953
1954
1955
1956
1957
1958
1959
1960
1961
1962
1963
1964
1965
1966
1967
1968
1969
1970
1971
1972
1973
1974
1975
1976
1977
1978
1979
1980
1981
1982
1983
1984
1985
1986
1987
1988
1989
1990
1991
1992
1993
1994
1995
1996
1997
1998
1999
2000
2001
2002
2003
2004
2005
2006

895 lines show locations of the interpreted seismic profiles with the type sections in Fig. 8
896 highlighted in red. (a) Top Basement; note especially the areas of maximum TWT depth
897 along the Stublick Fault (dark blue) indicating the areas of maximum throw of each original
898 fault segment, now linked by breached relay ramps (red circles); (b) Top Fell Sandstone
899 Formation (i.e. Top Lower Groups); (c) Top Tyne Limestone Formation; (d) Top Alston
900 Formation. Some areas have not been included in the maps because of the poor quality of
901 the seismic, especially in the western part of the study area.

902

Fig 10. Thickness maps of the interpreted formation intervals, interpolated from the 2D seismic
903 line interpretations (in TWT: 1 s equals approximately 1.5-2 km depending on the lithology).
904 Fault polygons show the fault loss areas for each package. (a) Lower Groups; (b) Tyne
905 Limestone Formation; (c) Alston Formation. Note especially the thickening of the Lower
906 Groups in (a) towards the west and south.

908

Fig 11. Schematic evolution model of the Northumberland Trough, including the timing and
909 the most likely location of the possible Early Carboniferous fault-related mineralisation at
910 depth; also shown is the suggestion of how the Permian vein-style mineralisation in the area
911 may be explained by (partial) remobilisation of this earlier mineralisation phase. The majority
912 of the interpreted faults are omitted for clarity. SF, Stublick Fault; NFF, Ninety-Fathom Fault;
913 ShF, Sweethope Fault; AF, Antonstown Fault. (a) Rifting initiates during the Courceyan, with
914 the structural high of the Alston Block forming in the south. (b) The main rifting continues into
915 the Chadian, with the syn-rift deposition of up to ≈ 2 km thick package of carbonate and
916 siliciclastic sediments. Stratabound base metal mineralisation within calcareous horizons may
917 form during this stage, similar to Irish Midlands, once sufficient strata have been deposited
918 (note that the possible mineralisation is not presented to real scale for illustration purposes).
919 Any Irish-type Pb-Zn mineralisation is likely to be confined to the vicinity of the Stublick Fault
920 in the southwestern part of the trough which represents deeper parts of the basin and may
921 contain more (shallow) marine sediments as most sub-aerial, siliciclastic material was sourced
922 from the north and the east. (c) Fault activity wanes from mid-Visean onwards (thermal
923 subsidence), with the deposition of post-rift sediments of the Yordale Group and younger. (d)
924 During the Permian, renewed minor extensional/transensional faulting and increased heat
925 flow trigger circulation of high-salinity, hot hydrothermal fluids within the trough. These may
926 partially leach and re-mobilize the Carboniferous Pb-Zn mineralisation at depth. A
927 Carboniferous seal (e.g. shale, evaporites) directs the bulk of the fluids towards and into the
928 Stublick Fault and the highly fractured Weardale Granite. Upwards percolation of these fluids
929 leads to near-surface deposition of veins within the Alston Block and southern Northumberland
930 Trough.

2007
2008
2009 932
2010
2011
2012
2013
2014
2015
2016
2017
2018
2019
2020
2021
2022
2023
2024
2025
2026
2027
2028
2029
2030
2031
2032
2033
2034
2035
2036
2037
2038
2039
2040
2041
2042
2043
2044
2045
2046
2047
2048
2049
2050
2051
2052
2053
2054
2055
2056
2057
2058
2059
2060
2061
2062
2063
2064
2065

2066
2067
2068
2069
2070
2071
2072
2073
2074
2075
2076
2077
2078
2079
2080
2081
2082
2083
2084
2085
2086
2087
2088
2089
2090
2091
2092
2093
2094
2095
2096
2097
2098
2099
2100
2101
2102
2103
2104
2105
2106
2107
2108
2109
2110
2111
2112
2113
2114
2115
2116
2117
2118
2119
2120
2121
2122
2123
2124

933 **References**

934 Anderson, I.K., Ashton, J.H., Boyce, A.J., Fallick, A.E., Russell, M.J. 1998. Ore depositional
935 processes in the Navan Zn-Pb deposit, Ireland. *Economic Geology* 93, 535-563.

936 Ashton, J.H., Blakeman, R.J., Geraghty, J.F., Beach, A., Collier, D., Philcox, M.E., Boyce, A.J.,
937 Wilkinson, J.J. 2015. The giant Navan carbonate-hosted Zn-Pb deposit: a review.
938 In: Archibald, S.M. & Piercey, S.J. (eds.) *Current Perspectives on Zinc Deposits*. Irish
939 Association for Economic Geology, Dublin, 85-122.

940 Ashton, J.H., Beach, A., Blakeman, R.J., Collier, D., Henry, P., Lee, R., Hitzman, M., Hope,
941 C., Huleatt-James, S., O'Donovan, B., & Philcox, M.N. 2018. Discovery of the Tara Deep
942 Zn-Pb Mineralization at the Boliden Tara Mine, Navan, Ireland: Success with Modern
943 Seismic Surveys. *SEG Special Publications* 21, 365–381.

944 Baba, M., Parnell, J., Bowden, S., Armstrong, J., Perez, M. & Wang, X., 2019. Emplacement
945 of oil in the Devonian Weardale Granite of northern England. *Proceedings of the Yorkshire
946 Geological Society* 62, 229-237.

947 Barrett, T.J., Anderson, G.M., 1988. The solubility of sphalerite and galena in 1-5 m NaCl
948 solutions to 300°C. *Geochimica Cosmochimica Acta* 52, 813-820.

949 Bateson, J.H., Johnson, C.C., Evans, A.D., 1983. Mineral reconnaissance in the
950 Northumberland Trough. *British Geological Survey Mineral Reconnaissance Programme
951 report* 62, 240 p.

952 Bott, M.H.P., Mason-Smith, D. 1957. The geological interpretation of a gravity survey of the
953 Alston Block and the Durham Coalfield. *Quarterly Journal of the Geological Society of
954 London* 113, 93-118.

955 Bott, M.H.P., Swinburn, P.M., Long, R.E. 1984. Deep structure and origin of the
956 Northumberland and Stainmore troughs. *Proceedings of the Yorkshire Geological Society
957* 44, 479-495.

958 Bott, M.H.P., Smith, F.W. 2018. The role of the Devonian Weardale Granite in the
959 emplacement of the North Pennine mineralization. *Proceedings of the Yorkshire Geological
960 Society* 62, 1-15.

961 Bouch, J.E., Naden, J., Shepherd, T.J., McKervery, J.A., Young, B., Benham, A.J., Sloane,
962 H.J., 2006. Direct evidence of fluid mixing in the formation of stratabound Pb-Zn-Ba-F
963 mineralisation in the Alston Block, North Pennine Orefield (England). *Mineralium Deposita*
964 41, 821-835.

965 Brown, G.C., Ixer, R.A., Plant, J.A., Webb, P.C. 1987. Geochemistry of granites beneath the
966 North Pennines and their role in mineralisation. *Transactions of the Institution of Mining and
967 Metallurgy Section B, Applied Earth Science* 96, B65-B76.

968 Burgess, I.C., Holliday, D.W. 1979. *Geology of the country around Brough-under-Stainmore.*
969 *Memoir of the Geological Survey of Great Britain, Sheet No. 31 (England and Wales).*

2125
2126
2127 970 Cann, J.R., Banks, D.A. 2001. Constraints on the genesis of the mineralization of the Alston
2128 Block, Northern Pennine Orefield, northern England. Proceedings of the Yorkshire
2129 971 Geological Society 53, 187-196.
2130 972
2131 973 Chadwick, R.A., Holliday, D.W. 1991. Deep crustal structure and Carboniferous basin
2132 974 development within the Iapetus Convergence Zone, northern England. Journal of the
2133 975 Geological Society of London 148, 41-53.
2134
2135 976 Chadwick, R.A., Holliday, D.W., Holloway, S., Hulbert, A.G. 1995. The Northumberland-
2136 977 Solway basin and adjacent areas. Subsurface memoir of the British Geological Survey,
2137 HMSO/NERC. 91 pp. ISBN 0118845012
2138
2139 978
2140 979 Collier, R.E.L., 1989. Tectonic evolution of the Northumberland Basin; the effects of renewed
2141 980 extension upon an inverted tectonic basin. Journal of the Geological Society, London 146,
2142 981 981-989.
2143
2144 982 Cowie, P.A., Gupta, S., Dawers, N.H. 2000. Implications of fault array evolution for synrift
2145 983 depocentre development: insights from a numerical fault growth model. Basin Research
2146 984 12, 241-261.
2147
2148 985 Crowley, S.F., Bottrell, S.H., McCarthy, M.D.B., Ward, J., Young, B. 1997. δ 34S of Lower
2149 986 Carboniferous anhydrite, Cumbria and its implications for barite mineralization in the
2150 987 northern Pennines. Journal of the Geological Society, London 154, 597-600.
2151
2152 988 Gallagher, M.J., Davies, A., Parker, M.E., Smith, R.T., Fortey, N.J., Easterbrook, G.D., 1977.
2153 989 Lead, zinc and copper mineralisation in basal Carboniferous sediments at Westwater,
2154 990 south Scotland. British Geological Survey Mineral Reconnaissance Programme report 17,
2155 991 142 p.
2156
2157 992 Gerhardstein, A.C., Brown, A.R., 1984. Interactive interpretation of seismic data. Geophysics
2158 993 49, 353-363.
2159
2160 994 Day, J.B.W. 1970. Geology of the country around Bewcastle. Memoir of the Geological Survey
2161 995 of Great Britain, Sheet 12 (England and Wales).
2162
2163 996 Dean, M.T., Browne, M.A.E., Waters, C.N., Powell, J.H. 2011. A lithostratigraphical framework
2164 997 for the Carboniferous successions of northern Great Britain (onshore). British Geological
2165 998 Survey, 165pp. (RR/10/007)
2166
2167 999 Dempsey, E. 2016. The North Pennines Orefield: a major regional phase of mantle sourced
2168 1000 mineralisation and transtension during the earliest Permian. Proceedings of the OUGS 2,
2169 1001 33-37.
2170
2171 1002 De Paola, N., Holdsworth, R.E., McCaffrey, K.J.W., Barchi, M.R., 2005. Partitioned
2172 1003 transtension: an alternative to basin inversion models. Journal of Structural Geology 27,
2173 1004 607-625.
2174
2175
2176
2177
2178
2179
2180
2181
2182
2183

2184
2185
2186 1005 Dunham, K.C. 1983. Ore genesis in the English Pennines: a fluoritic subtype. In: Kisvarsanyi,
2187 G., Grant, S.K., Pratt, W.P. & Koenig, J.W. (eds.) International conference on Mississippi
2188 1006 Valley type lead-zinc deposits. University of Missouri. Rolla Press, 86-112.
2189 1007
2190
2191 1008 Dunham, K.C. 1988. Pennine mineralization in depth. Proceedings of the Yorkshire Geological
2192 1009 Society 47, 1-12.
2193
2194 1010 Dunham, K.C. 1990. Geology of the Northern Pennine Orefield, Volume 1 Tyne to Stainmore
2195 1011 (2nd Ed.). Economic Memoir of the British Geological Survey, sheets 19 and 25 and parts
2196 1012 of 13, 24, 26, 31, 32 (England and Wales).
2197
2198 1013 Dunham, K.C., Bott, M.H.P., Johnson, G.A.L., Hodge, B.L. 1961. Granite beneath the Northern
2199 1014 Pennines (England). Report 19th International Geology Congress, London, part 4, 46-63.
2200
2201 1015 Everett., C.E., Wilkinson J.J., Rye, D.M., 1999. Fracture-controlled fluid flow in the Lower
2202 1016 Palaeozoic basement rocks of Ireland: implication for the genesis of Irish-type Zn-Pb
2203 deposits. In: McCaffrey, K.J.W., Lonergan, L. and Wilkinson, J.J. (Eds.) Fractures, fluid
2204 1017 flow, and mineralization. Geological Society, London, Special Publications, 155, 247-276.
2205 1018
2206
2207 1019 Fraser, A. J., & Gawthorpe, R. L. (1990). Tectono-stratigraphic development and hydrocarbon
2208 1020 habitat of the Carboniferous in northern England. Geological Society, London, Special
2209 Publications, 55(1), 49-86.
2210 1021
2211 1022 Fraser, A.J., Gawthorpe, R.L. 2003. An atlas of Carboniferous basin evolution in northern
2212 1023 England. Geological Society Memoir 28.
2213
2214 1024 Gibson, G.M., Meixner, A.J., Withnall, I.W., Korsch, R.J., Hutton, L.J., Jones, L.E.A.,
2215 1025 Holzschuh, J., Costelloe, R.D., Henson, P.A., Saygin, E., 2016. Basin architecture and
2216 evolution in the Mount Isa mineral province, northern Australia: Constraints from deep
2217 1026 seismic reflection profiling and implications for ore genesis. Ore Geology Reviews 76, 414-
2218 1027 441.
2219
2220 1028
2221 1029 Haszeldine, R.S. 1984. Muddy deltas in freshwater lakes, and tectonism in the Upper
2222 Carboniferous Coalfield of NE England. Sedimentology 31, 811-822.
2223 1030
2224 1031 Hitzman, M.W. 1999. Extensional faults that localize Irish syndiagenetic Zn-Pb deposits and
2225 their reactivation during Variscan compression. In: McCaffrey, K.J.W., Lonergan, L. &
2226 1032 Wilkinson, J.J. (eds.) Fractures, Fluid Flow and Mineralization. Geological Society, London,
2227 1033 Special Publications, 155, 233-245.
2228
2229 1034
2230 1035 Hitzman, M.W., Large, D. 1986. A review and classification of the Irish carbonate-hosted base
2231 1036 metal deposits. In: Andrew, C.J., Crowe, R.W.A., Finlay, S., Pennell, W.M. & Pyne, J.F.
2232 (eds.) Geology and Genesis of Mineral Deposits in Ireland. Irish Association for Economic
2233 1037 Geology, Dublin, 217-238.
2234 1038
2235
2236 1039 Hitzman, M.W., Beaty, D.W. 1996. The Irish Zn-Pb-(Ba) Orefield. Society of Economic
2237 1040 Geologists Special Publication 4, 112-143.
2238
2239
2240
2241
2242

2243
2244
2245 1041 Holliday, D.W., Pattison, J. 1990. Carboniferous geology of Corbridge and Prudhoe:
2246 Geological notes and local details for sheets NZ06 and the eastern parts of NY96NE and
2247 1042 SE (Northumberland). British Geological Survey Technical Report, WA/90/13.
2248 1043
2249
2250 1044 Hu, Y., Liu, W., Wang, J., Zhang, G., Zhou, Z., Han, R., 2017. Basin-scale structure control of
2251 1045 Carlin-style gold deposits in central Southwestern Guizhou, China: Insights from seismic
2252 reflection profiles and gravity data. *Ore Geology Reviews* 91, 444-462.
2253 1046
2254 1047 Hudson, R.G.S., 1924. On the rhythmic succession of the Yoredale series in Wensleydale.
2255 Proceedings of the Yorkshire Geological Society 20, 125-135.
2256 1048
2257 1049 Jackson, S.A., Beales, F.W. 1967. An aspect of sedimentary basin evolution: the
2258 concentration of Mississippi Valley type ores during late stage of diagenesis. *Canadian*
2259 1050 *Petroleum Geology Bulletin* 15, 383-433.
2260 1051
2261 1052 Johnson, G.A.L. 1980. The Carboniferous Dinantian and Namurian rocks. In: Robson, D.A.
2262 (ed.) *The geology of north east England*. Newcastle upon Tyne: Natural History Society of
2263 1053 Northumbria, 11-23.
2264 1054
2265
2266 1055 Jones, D.G., Plant, J.A., Colman, T.B. 1994. The genesis of the Pennine Mineralization of
2267 1056 Northern England and its relationship to mineralization in central Ireland. In: Fontbote, L.
2268 & Boni, M. (eds.) *Sediment-hosted Zn-Pb Ores*, Springer Heidelberg, 198-218.
2269 1057
2270 1058 Kimbell, G.S., Chadwick, R.A., Holliday, D.W., Werngren, O.C. 1989. The structure and
2271 evolution of the Northumberland Trough from new seismic reflection data and its bearing
2272 1059 on modes of continental extension. *Journal of the Geological Society of London* 146, 775-
2273 1060 787.
2274 1061
2275
2276 1062 Kimbell, G.S., Young, B., Millward, D., Crowley, Q.G., 2010. The North Pennine Batholith
2277 (Weardale Granite) of northern England: new data on its age and form. *Proceedings of the*
2278 1063 *Yorkshire Geological Society* 58, 107-128.
2279 1064
2280 1065 Kraemer, D., Viehmann, S., Banks, D., Sumoondur, A.D., Koeberl, C., Bau, M. 2019. Regional
2281 variations in fluid formation and metal sources in MVT mineralization in the Pennine
2282 1066 Orefield, UK: Implications from rare earth element and yttrium distribution, Sr-Nd isotopes
2283 1067 and fluid inclusion compositions of hydrothermal vein fluorites. *Ore Geology Reviews* 107,
2284 1068 960-972.
2285 1069
2286
2287 1070 Kyne, R., Torremans, K., Güven, J., Doyle, R., Walsh, J., 2019. 3-D modeling of the Lisheen
2288 and Silevermines deposits, County Tipperary, Ireland: Insights into structural controls on
2289 1071 the formation of Irish Zn-Pb deposits. *Economic Geology* 114, 93-116.
2290 1072
2291
2292 1073 Leach, D.L., Bradley, D., Lewchuck, M.T., Symons, D.T.A., de Marsily, G., Brannon, J., 2001.
2293 1074 Mississippi Valley-type lead-zinc deposits through geological time: implication from recent
2294 age-dating research. *Mineralium Deposita* 36, 711-740.
2295 1075
2296 1076 Leeder, M.R. 1973. Sedimentology and palaeogeography of the Upper Old Red Sandstone in
2297 the Scottish Border Basin. *Scottish Journal of Geology* 9, 117-144.
2298 1077
2299
2300
2301

2302
2303
2304 1078 Leeder, M.R. 1974. The origin of the Northumberland Basin. *Scottish Journal of Geology* 10,
2305 283-296.
2306 1079
2307 1080 Leeder, M.R. 1982. Upper Paleozoic basins of the British Isles- Caledonide inheritance versus
2308 Hercynian plate margin processes. *Journal of the Geological Society of London* 139, 479-
2309 1081 491.
2310 1082
2311
2312 1083 Leeder, M.R., Fairhead, D., Lee, A., Stuart, G., Clemmey, H., Al-Haddeh, B., Green, C. 1989.
2313 1084 Sedimentary and tectonic evolution of the Northumberland Basin. In: Arthurton, R.S.,
2314 1085 Gutteridge, P. & Nolan, S.C. (eds.) *The role of tectonics in Devonian and Carboniferous*
2315 1086 *sedimentation in the British Isles*. Leeds: Yorkshire Geological Society, 207-223.
2316 1086
2317 1087 Lewis, H., Couples, G.D. 1999. Carboniferous basin evolution of central Ireland – simulation
2318 1088 of structural controls on mineralization. In: McCaffrey, K.J.W., Lonergan, L. & Wilkinson,
2320 1089 J.J. (eds.) *Fractures, Fluid Flow and Mineralization*. Geological Society, London, Special
2321 1090 Publications 155, 277-302.
2322 1090
2323 1091 Matte, P. 1986. Tectonics and plate tectonic model for the Variscan Belt of Europe.
2324 1092 *Tectonophysics* 126, 329-374.
2325 1092
2326 1093 Max, M.D., Ryan, P.D., Inamdar, D.D. 1983. A magnetic deep structural geology interpretation
2327 1094 of Ireland. *Tectonics* 2, 431-451.
2328 1094
2329 1095 McKenzie, D.P. 1978. Some remarks on the development of sedimentary basins. *Earth and*
2330 1096 *Planetary Science Letters* 40, 25-32.
2331 1096
2332 1097 McKerrow, W.S., Mac Niocaill, C., Dewey, J.F. 2000. The Caledonian Orogeny redefined.
2333 1098 *Journal of the Geological Society of London* 157, 1149-1154.
2334 1098
2335 1099 Milkereit, B., Eaton, D., Wu, J., Perron, G., Salisbury, M., Berrer, E.K., Morrison, G., 1996.
2336 1100 *Economic Geology* 91, 829-834.
2337 1100
2338 1101 Nance, R.D., Gutiérrez-Alonso, G., Keppie, J.D., Linnemann, U., Murphy, J.D., Quesada, C.,
2339 1102 Strachan, R.A., Woodcock, N.H. 2012. A brief history of the Rheic Ocean. *Geoscience*
2340 1103 *Frontiers* 3, 125-135.
2341 1103
2342 1104 O'Reilly, B.M., Readman, P.W., Murphy, T. 1999. Gravity lineaments and carboniferous-
2343 1105 hosted base metal deposits of the Irish Midlands. In: McCaffrey, K.J.W., Lonergan, L. &
2344 1106 Wilkinson, J.J. (eds.) *Fractures, fluid flow and mineralization*. Geological Society London
2345 1107 *Special Publications* 155, 313-321.
2346 1107
2347 1108 Philcox, M.E. 1984. Lower Carboniferous lithostratigraphy of the Irish Midlands. *Irish*
2348 1109 *Association for Economic Geology*, Dublin.
2349 1109
2350 1110 Plant, J.A., Jones, D.G., Brown, G.C., Colman, T.B., Conrwell, J.S., Smith, N.J.P., Walker,
2351 1111 A.S.D., Webb. P.C., 1988. Metallogenic models and exploration criteria for buried
2352 1112 carbonate-hosted ore deposits: results of a multidisciplinary study in eastern England. In:
2353 1113 Boissonnas, J., Omenetto, P. (eds) *Mineral Deposits within the European Community*.
2354 1114 *Society for Geology Applied to Mineral Deposits*, Special Publication 6, 321-352.
2355 1114
2356 1114
2357 1114
2358
2359
2360

2361
2362
2363 1115 Shearley, E., Hitzman, M.W., Walton, G., Redmond, P., Davis, R., King, M., Duffy, L.,
2364 Goodman, R. 1992. Structural controls of mineralization, Lisheen Zn-Pb-Ag deposit, Co.
2365 1116 Tipperary, Ireland. Geological Society of America, Abstracts with Programs 24, A354.
2366 1117
2367
2368 1118 Smith, R.T., Walker, A.S.D., Bland, D.J., 1996. Mineral investigations in the Northumberland
2369 1119 Trough: Part 1, Arnton Fell area, Borders, Scotland. British Geological Survey Mineral
2370 Reconnaissance Programme report 18, 49 p.
2371 1120
2372 1121 Stone, P., Millward, D., Young, B., Meritt, J.W., Clarke, S.M., McCormac, M., Lawrence, D.J.D.
2373 1122 2010. British Regional Geology: Northern England (5th Ed.). British Geological
2374 Survey, Keyworth, Nottingham.
2375 1123
2376 1124 Taylor, S. 1984. Structural and palaeogeographic controls of lead-zinc mineralization in the
2377 Silvermines orebodies, Republic of Ireland. Economic Geology 79, 529-548.
2378 1125
2379 1126 Torremans, K., Kyne, R., Doyle, R., Güven, J.F., Walsh, J., 2018. Controls on metal
2380 distributions at the Lisheen and Silvermines deposits: insights into fluid flow pathways in
2381 1127 Irish-type Zn-Pb deposits. Economic Geology 113, 1455-1477.
2382 1128
2383 1129 Torsvik, T.H., Smethurst, M.A., Meert, J.G., Van der Voo, R., McKerrow, W.S., Brasier, M.D.,
2385 1130 Sturt, B.A., Walderhaug, H.J. 1996. Continental break-up and collision in the
2386 Neoproterozoic and Paleozoic – A tale of Baltica and Laurentia. Earth-Science Reviews
2387 1131 40, 229-258.
2388 1132
2389 1133 Treagus, J.E., 1992. Caledonian Structures in Britain: south of the Midland Valley, Geological
2390 Conservation Review Series, No.3, Chapman and Hall, London, 177 p.
2391 1134
2392 1135 Tucker, M., Gallagher, J., Lemon, K., Leng, M., 2003. The Yoredale cycles of Northumbria:
2393 high-frequency clastic-carbonate sequences of the Mid-Carboniferous icehouse world.
2394 1136 OUGS Journal 24, 5-10.
2395 1137
2396 1138 Wagner, T., Boyce, A.J., 2001. Sulphur isotope characteristics of recrystallisation,
2398 1139 remobilisation and reaction processes: a case study from the Ramsbeck Pb-Zn deposit,
2399 Germany. Mineralium Deposita 36, 670-679.
2400 1140
2401 1141 Walsh, J.J., Torremans, K., Guven, J., Kyne, R., Conneally, J., Bonson, C. 2018. Fault
2402 controlled fluid flow within extensional basins and its implications for sediment-hosted
2403 1142 mineral deposits. Society of Economic Geologists Special Publications 21, 237-269.
2404 1143
2405 1144 Wilkinson, J.J. 2010. A review of fluid inclusion constraints on mineralization in the Irish
2407 1145 orefield and implications for the genesis of sediment-hosted Zn-Pb deposits. Economic
2408 Geology 105, 417-442.
2409 1146
2410 1147 Wilkinson, J.J., Hitzman, M.W. 2015. The Irish Zn-Pb orefield: The view from 2014. In:
2411 1148 Archibald, S.M., Piercey, S.J. (eds.) Current Perspectives on Zinc Deposits. Irish
2413 1149 Association for Economic Geology, Dublin, 59-72.
2414
2415
2416
2417
2418
2419

2420
2421
2422
2423
2424
2425
2426
2427
2428
2429
2430
2431
2432
2433
2434
2435
2436
2437
2438
2439
2440
2441
2442
2443
2444
2445
2446
2447
2448
2449
2450
2451
2452
2453
2454
2455
2456
2457
2458
2459
2460
2461
2462
2463
2464
2465
2466
2467
2468
2469
2470
2471
2472
2473
2474
2475
2476
2477
2478

1150 Williams, B., Brown, C., 1986. A model for the genesis of Zn-Pb deposits in Ireland In: Andrew,
1151 C.J., Crowe, R.W.A., Finlay, S., Pennells, W.M., Pyne, J.F. (Eds.) Geology and genesis of
1152 mineral deposits in Ireland. Irish Association of Economic Geology, 579–590.

A) BEFORE FAULTING

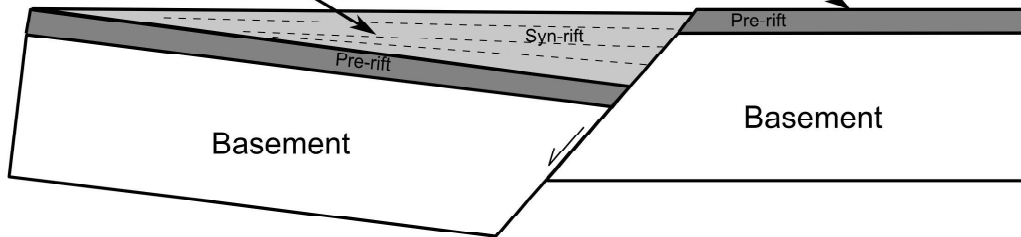
Pre-rift sediments deposited onto basement - no significant thickness changes



B) DURING FAULTING

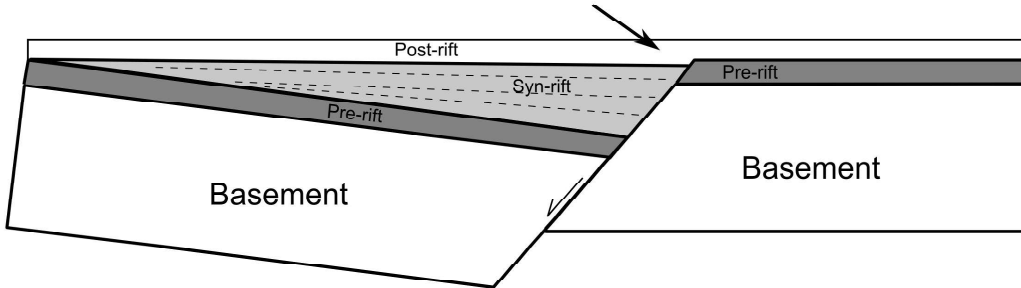
Syn-rift sediments deposited onto the hanging-wall - thickness of the package increases towards the fault

Thinner syn-rift or non-deposition onto footwall



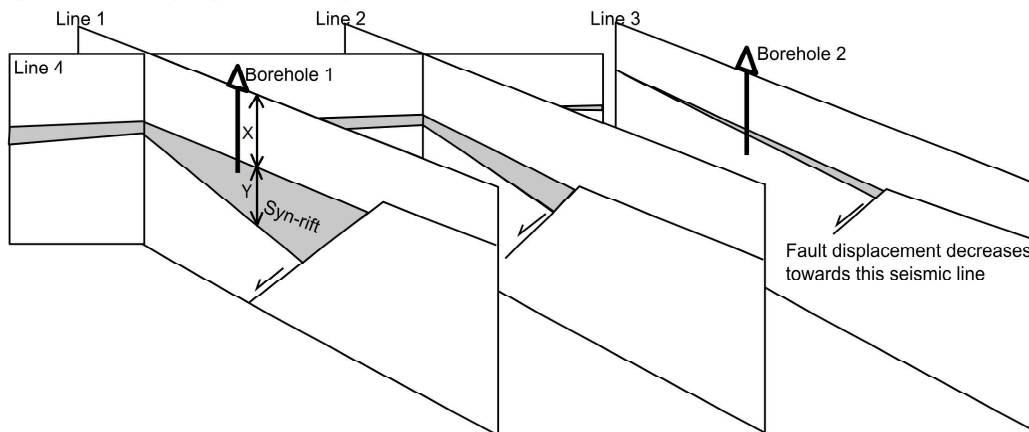
C) AFTER FAULTING

Post-rift sediments deposited across the area - minor thickness changes may exist if rift basin not completely filled during rifting



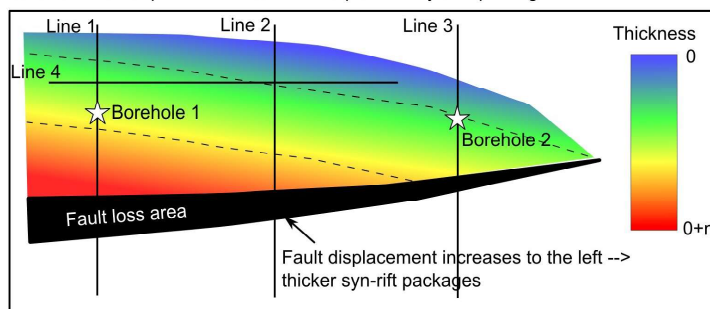
D) METHOD

A grid of 2D seismic lines is interpreted for faults and pre-, syn-, and post-rift packages (only basement and syn-rift shown below). Any borehole (well) information will constrain the depths of formation boundaries.



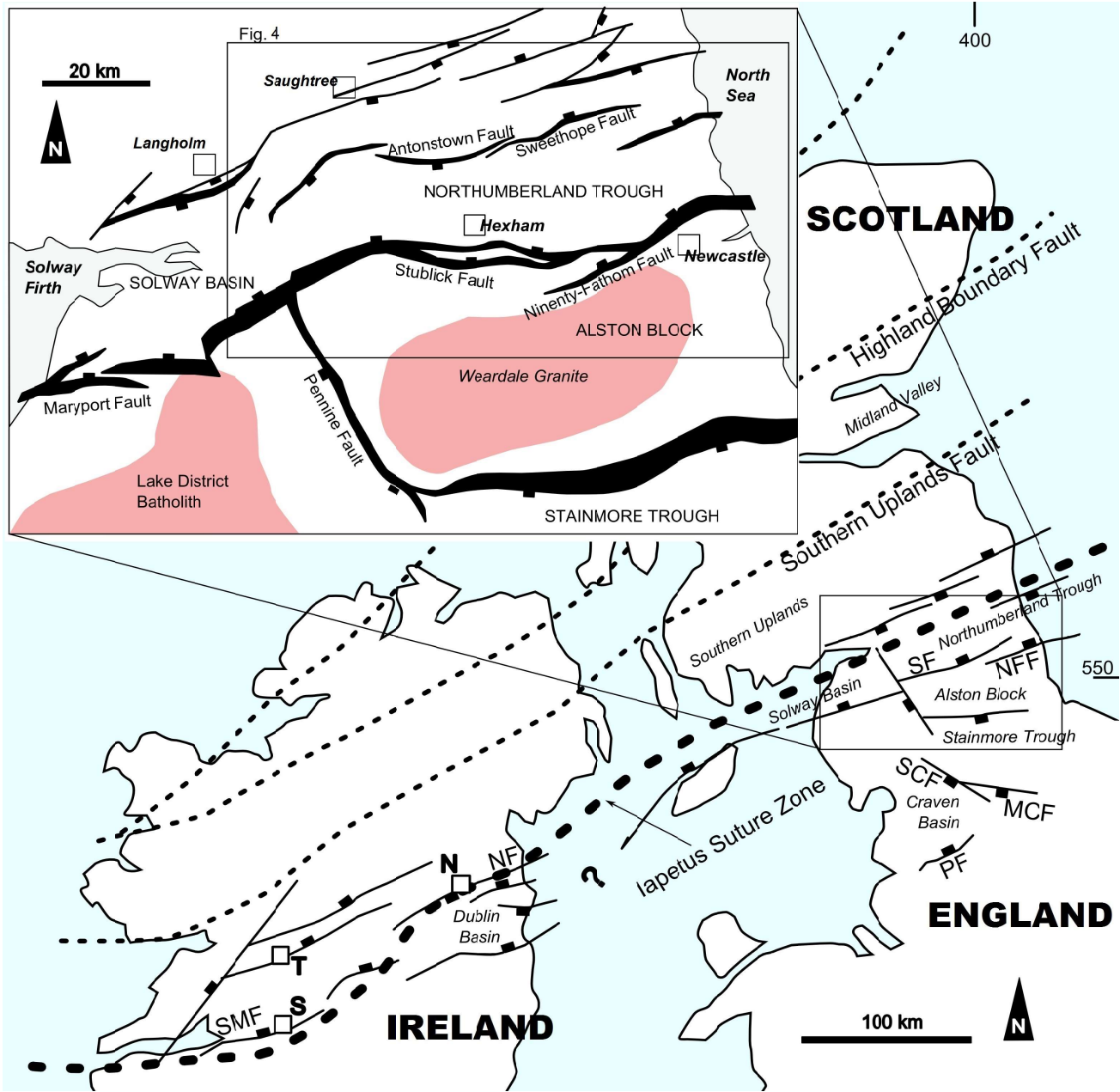
The 2D interpretations can then be interpolated to '3D' (2.5D) interpretations of e.g. the sedimentary package thicknesses (right) or basement/formation top topography/structures, in order to further investigate the spatial distribution of the structures and the syn-faulting sedimentary packages.

MAP VIEW: interpreted 3D thickness map for the syn-rift package

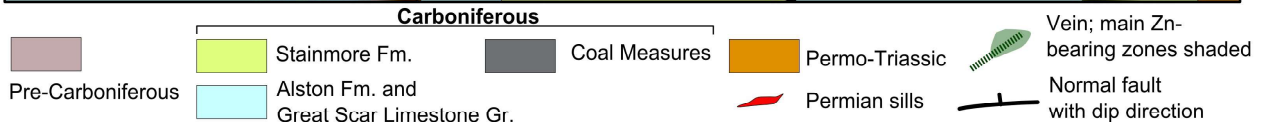
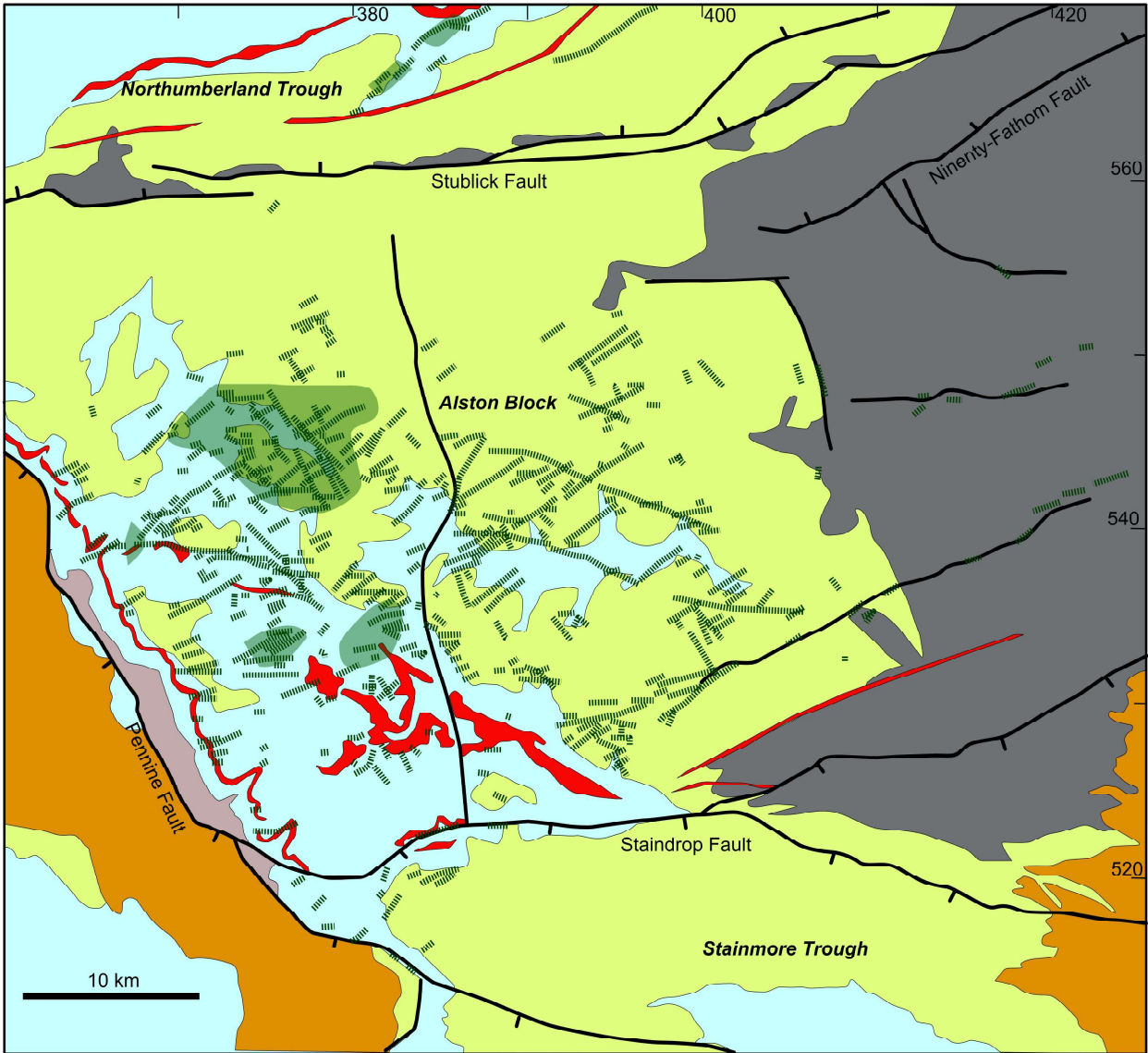


1
2
3
4
5
6
7
8
9
10
11
12
13
14
15
16
17
18
19
20
21
22
23
24
25
26
27
28
29
30
31
32
33
34
35
36
37
38
39
40
41
42
43
44
45
46
47
48
49
50
51
52
53
54
55

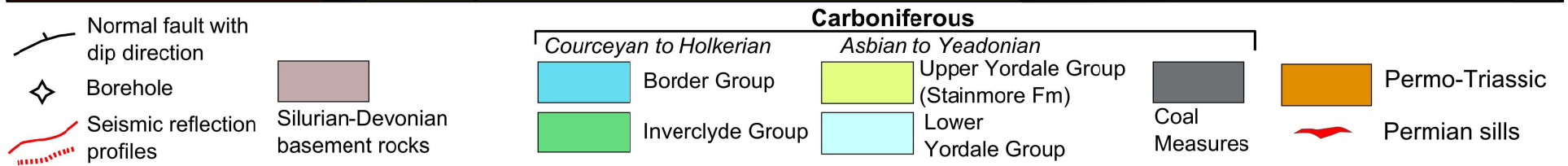
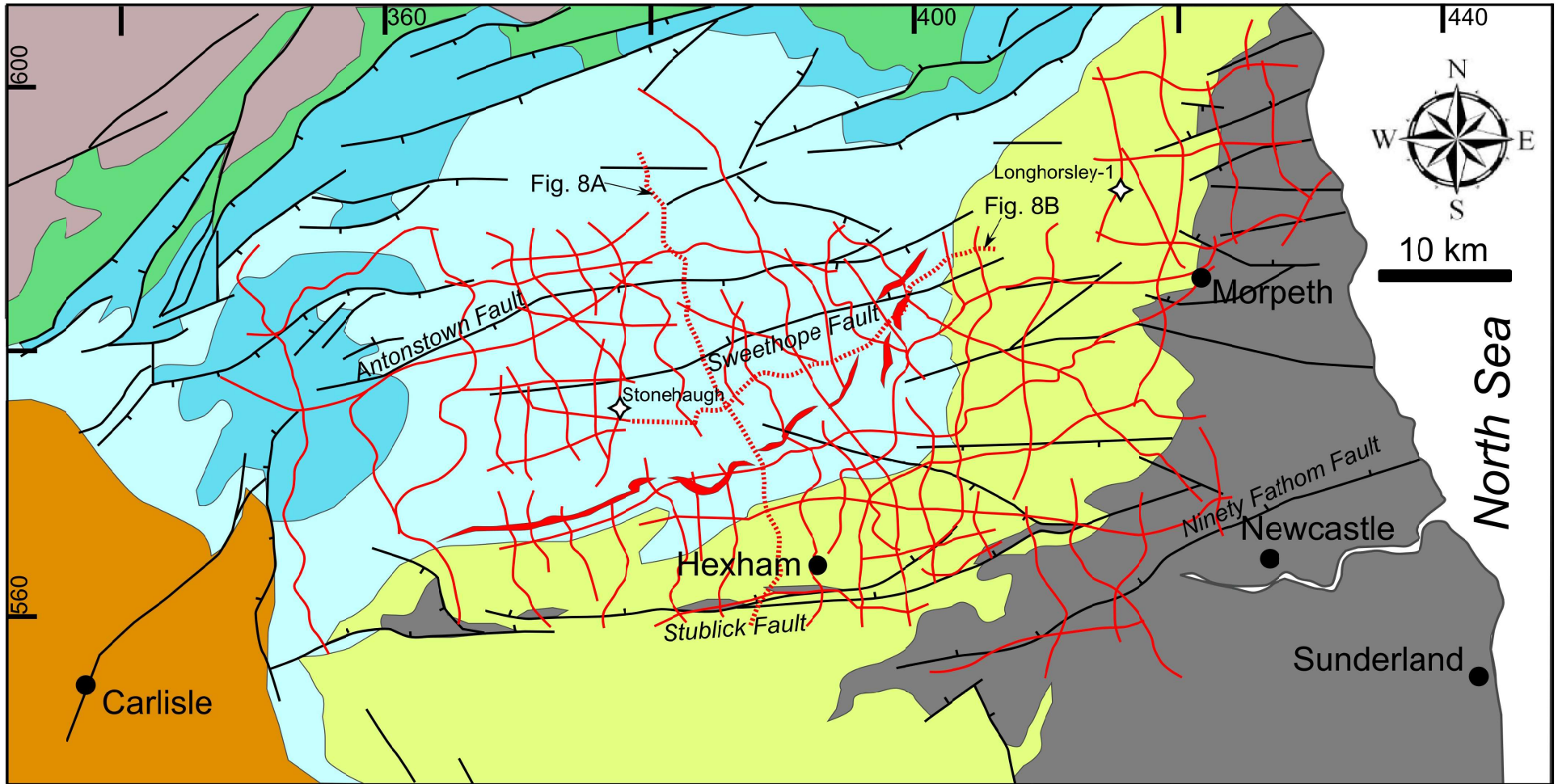
1
2
3
4
5
6
7
8
9
10
11
12
13
14
15
16
17
18
19
20
21
22
23
24
25
26
27
28
29
30
31
32
33
34
35
36



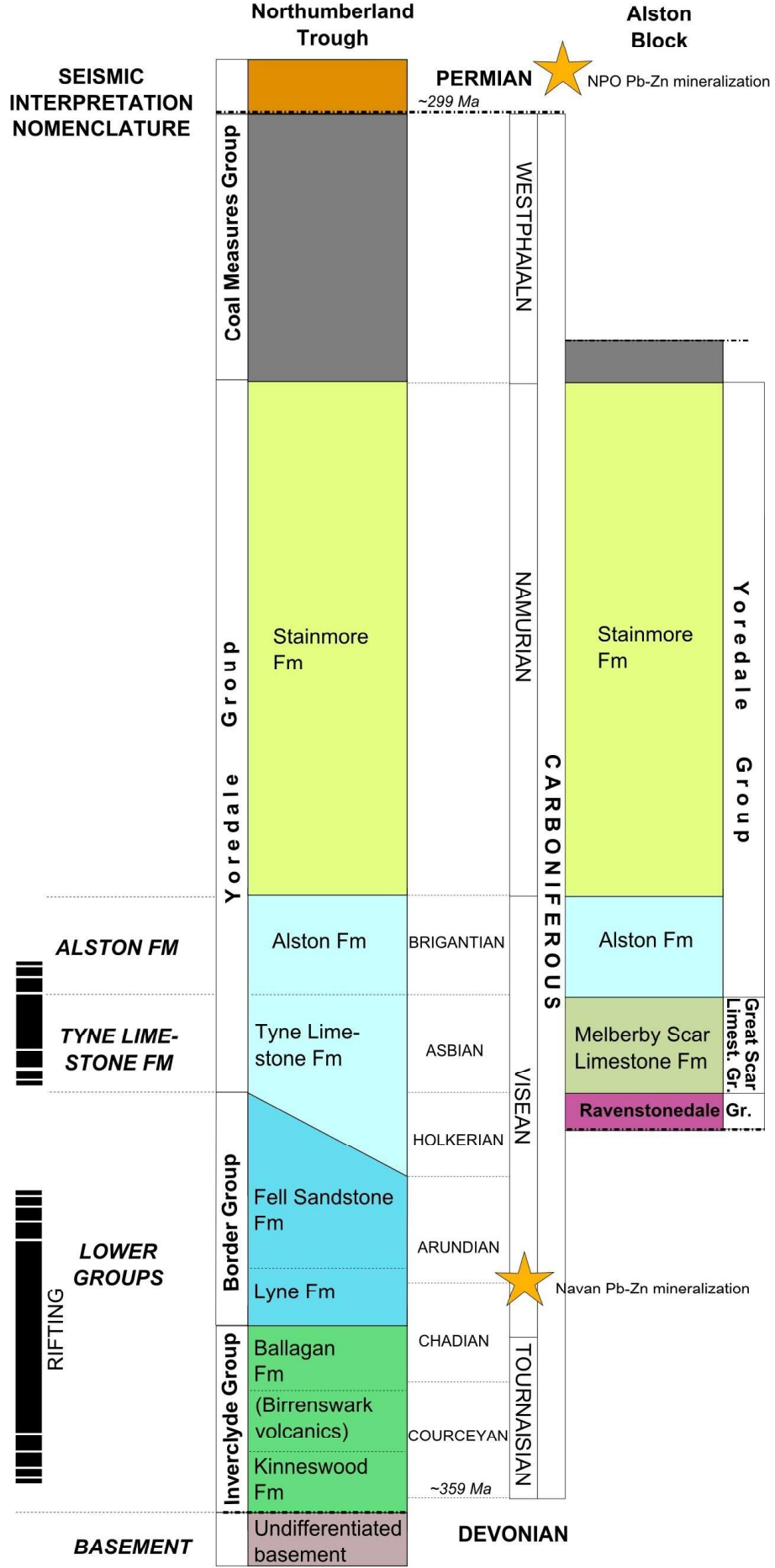
1
2
3
4
5
6
7
8
9
10
11
12
13
14
15
16
17
18
19
20
21
22
23
24
25
26
27
28
29
30
31
32
33
34
35
36
37
38
39
40
41
42
43
44
45
46
47
48
49
50
51
52
53
54
55



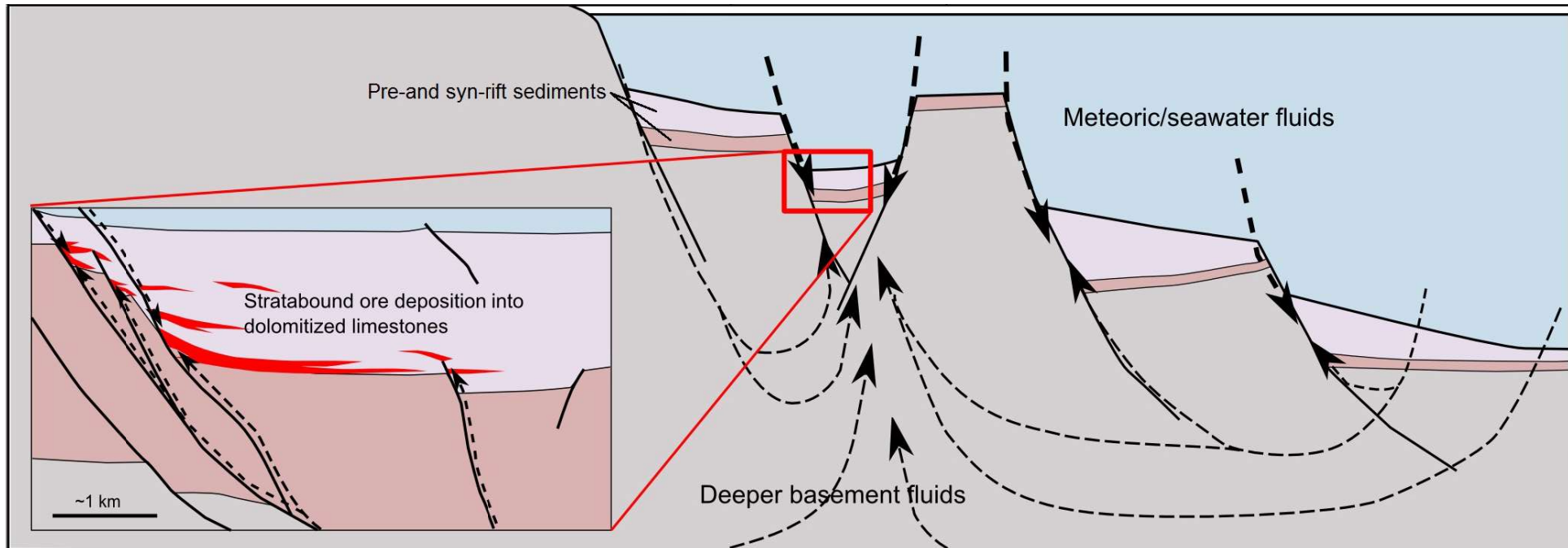
1
2
3
4
5
6
7
8
9
10
11
12
13
14
15
16
17
18
19
20
21
22
23
24
25
26
27
28
29
30
31
32
33
34
35
36



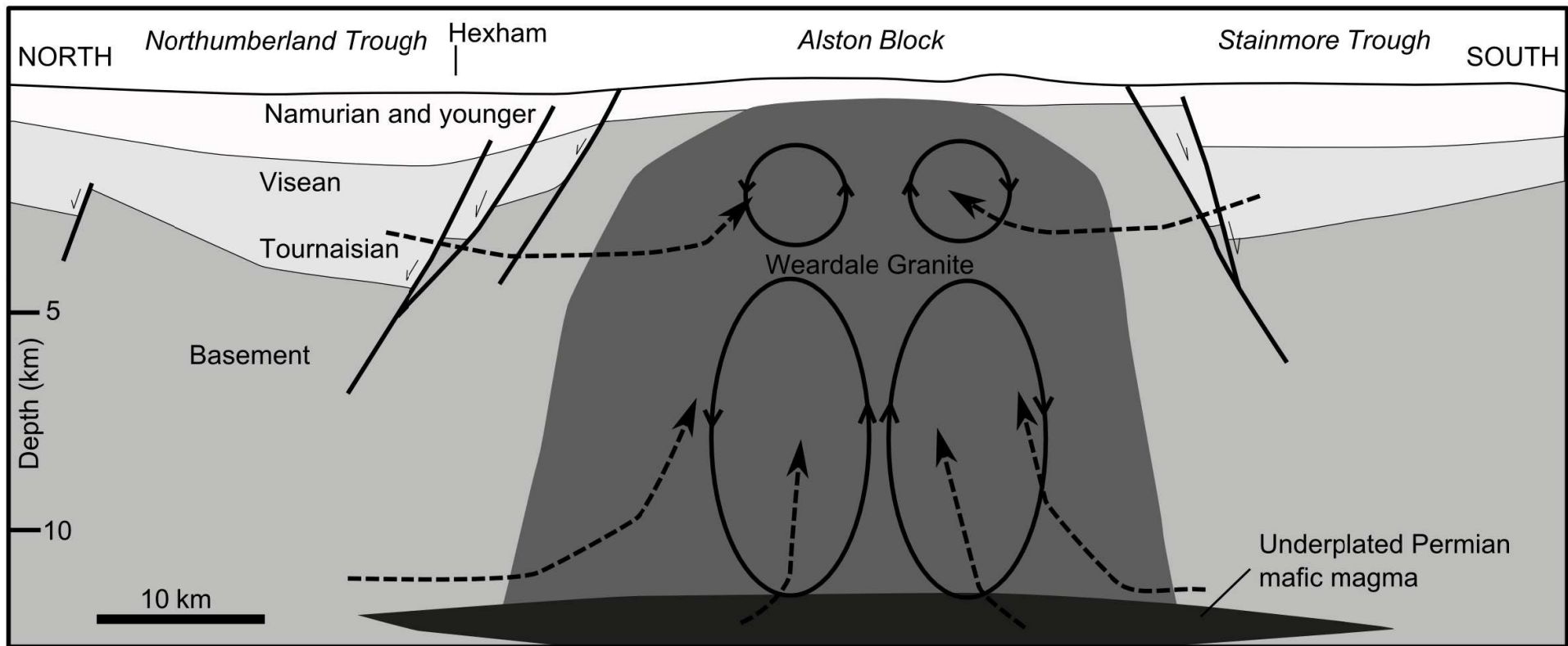
1
2
3
4
5
6
7
8
9
10
11
12
13
14
15
16
17
18
19
20
21
22
23
24
25
26
27
28
29
30
31
32
33
34
35
36
37
38
39
40
41
42
43
44
45
46
47
48
49
50
51
52
53
54
55

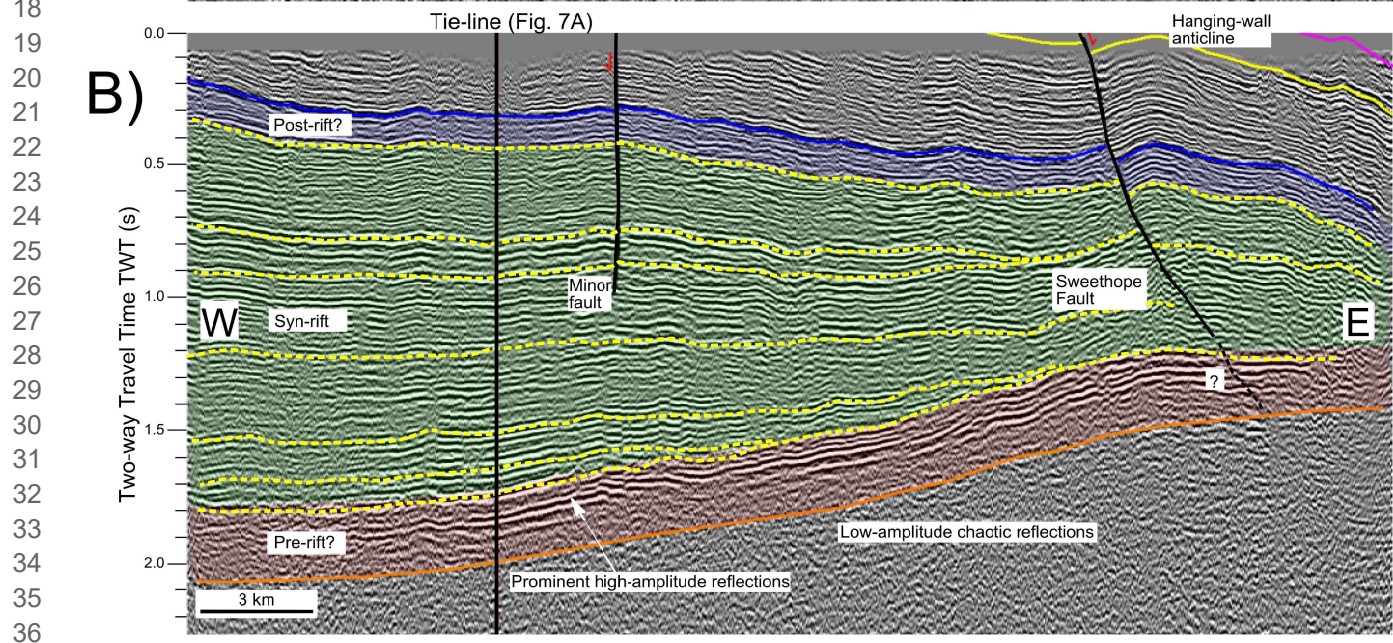
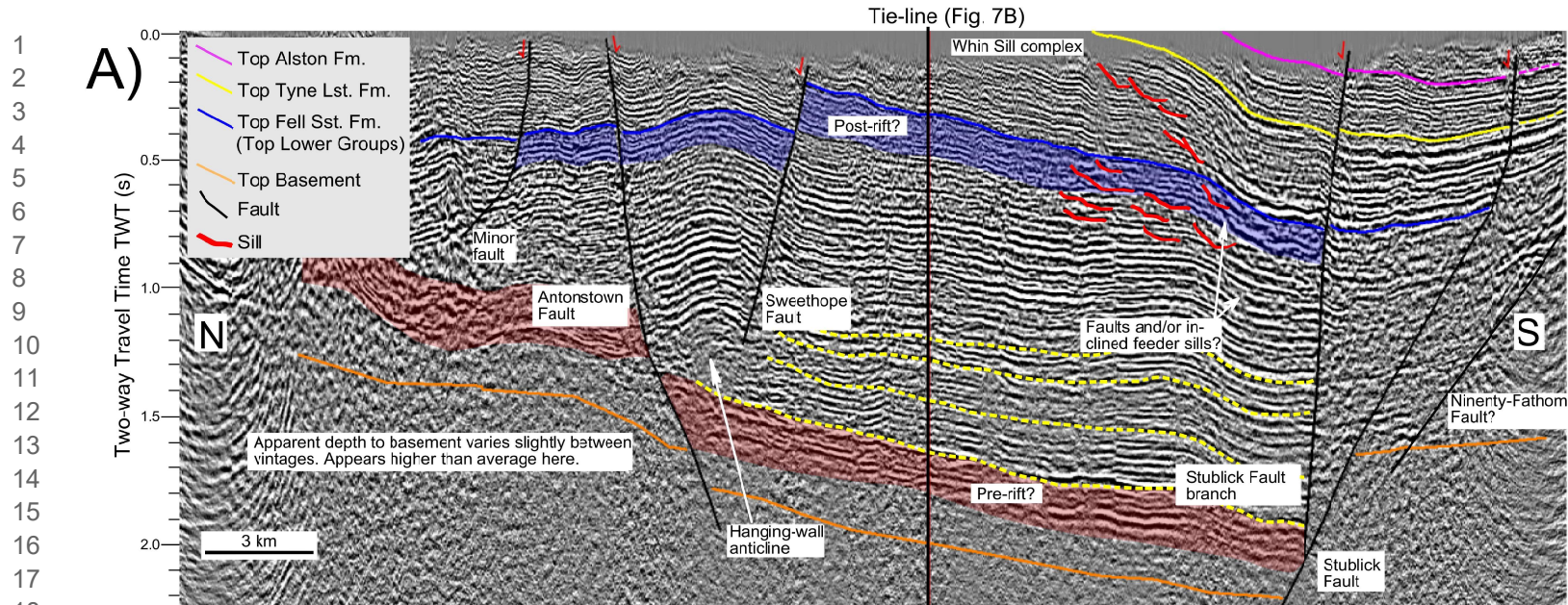


1
2
3
4
5
6
7
8
9
10
11
12
13
14
15
16
17
18
19
20
21
22
23
24
25
26
27
28
29
30
31
32
33
34
35
36

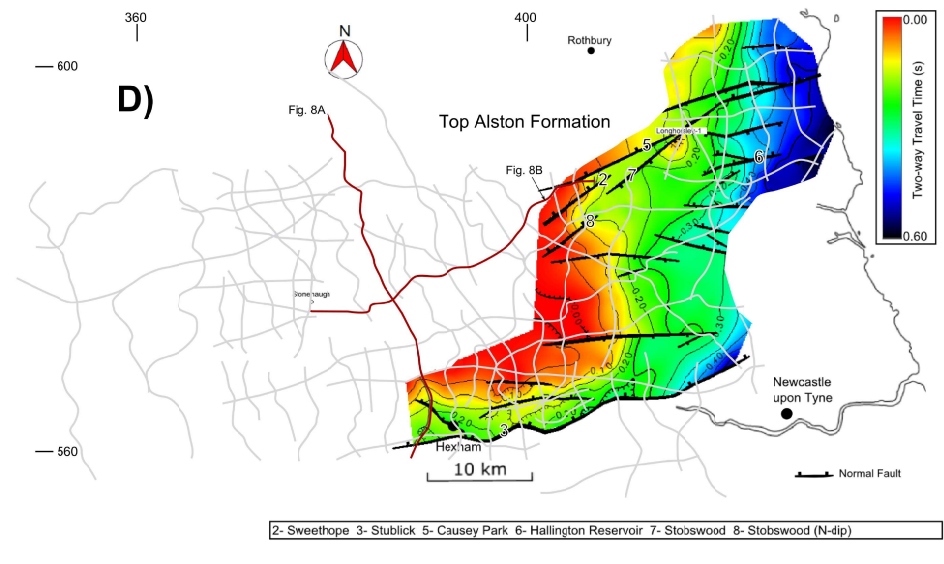
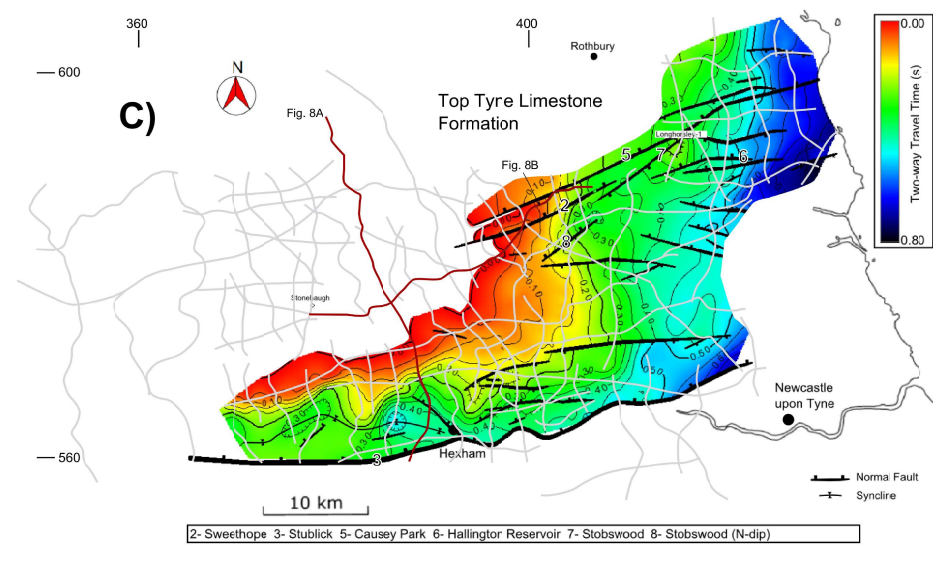
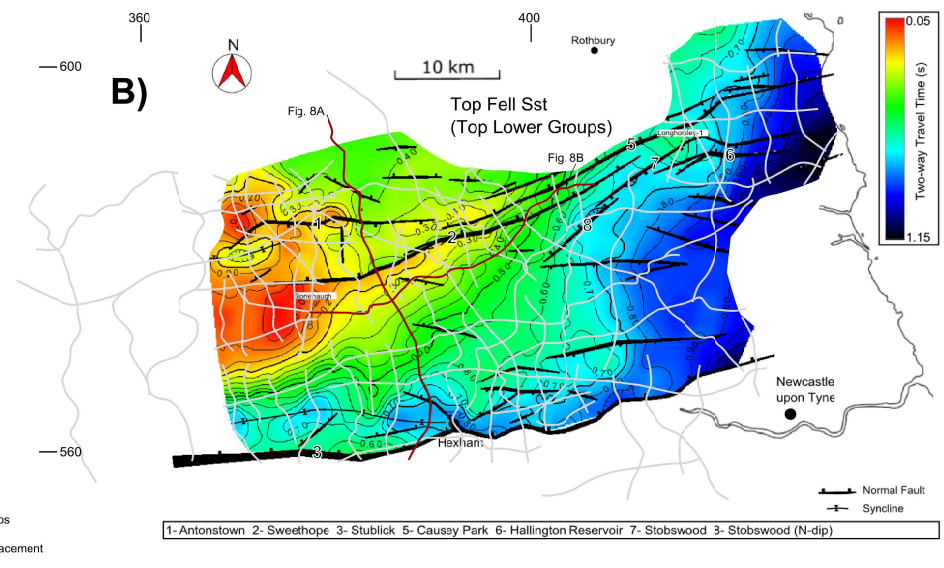
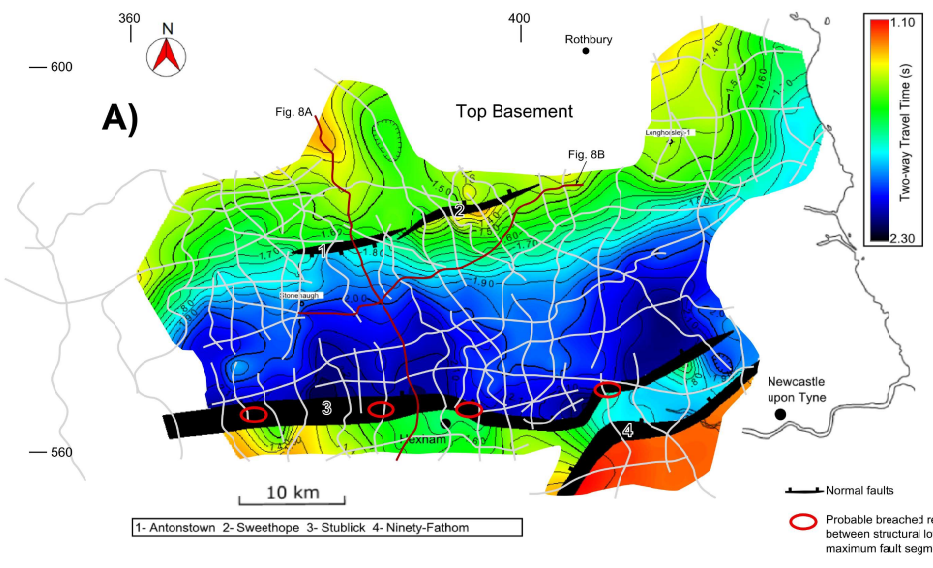


1
2
3
4
5
6
7
8
9
10
11
12
13
14
15
16
17
18
19
20
21
22
23
24
25
26
27
28
29
30
31
32
33
34
35
36

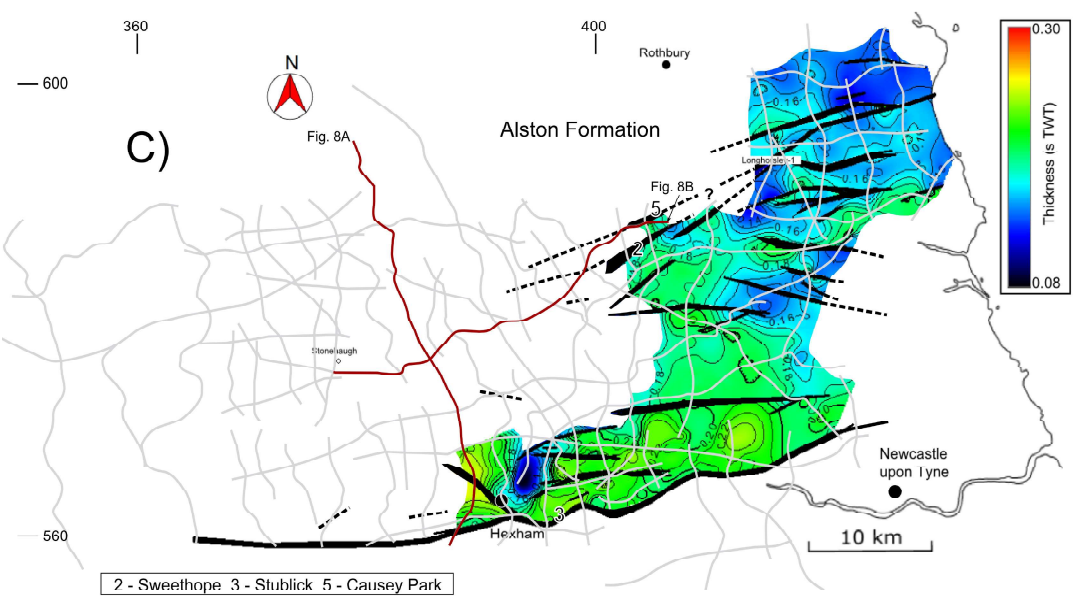
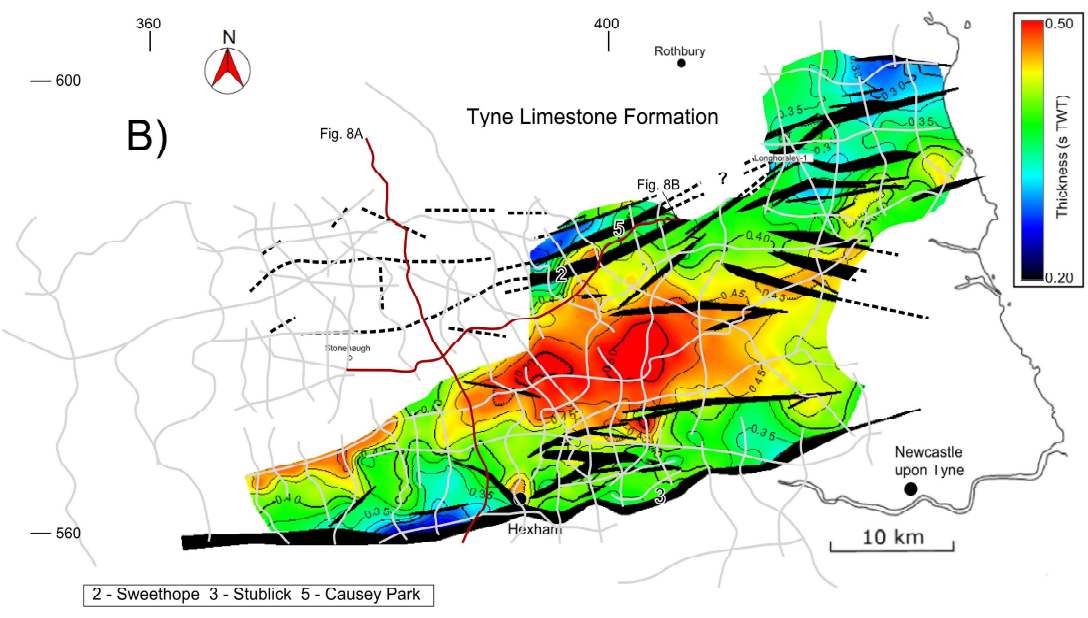
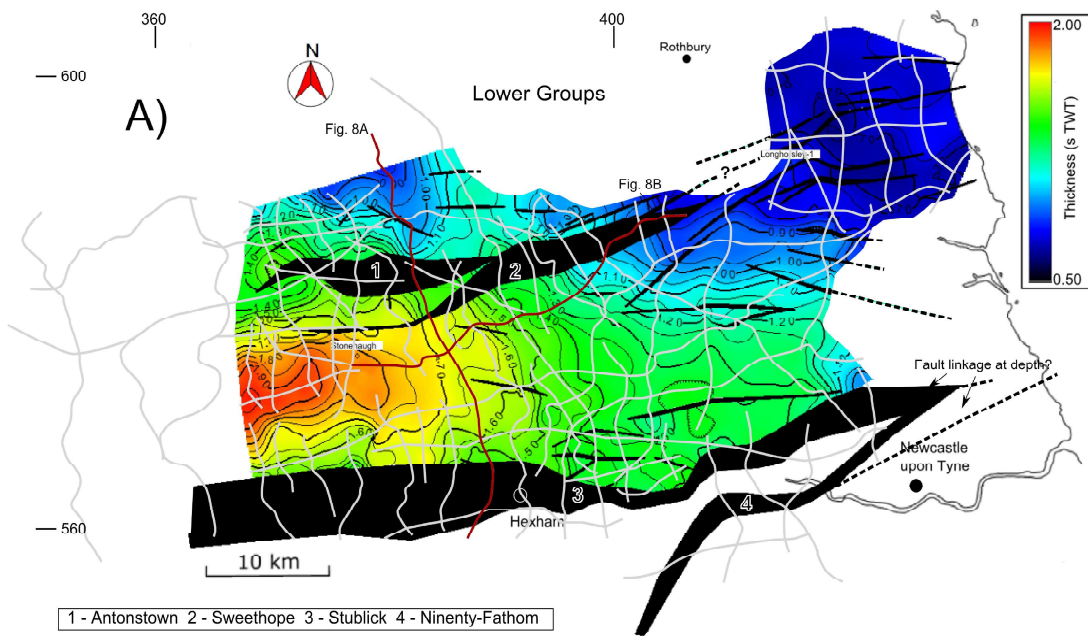




1
2
3
4
5
6
7
8
9
10
11
12
13
14
15
16
17
18
19
20
21
22
23
24
25
26
27
28
29
30
31
32
33
34
35
36



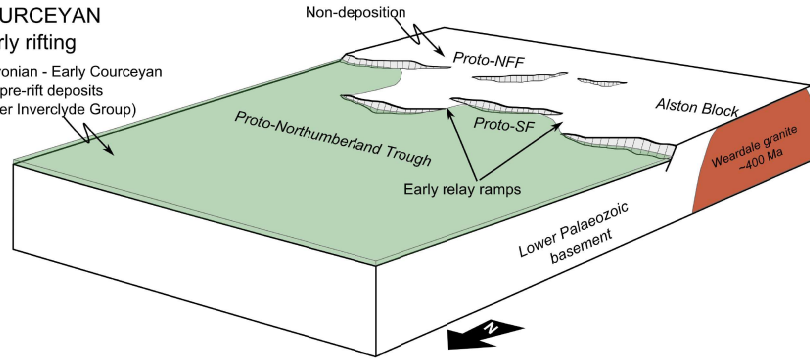
1
2
3
4
5
6
7
8
9
10
11
12
13
14
15
16
17
18
19
20
21
22
23
24
25
26
27
28
29
30
31
32
33
34
35
36
37
38
39
40
41
42
43
44
45
46
47
48
49
50
51
52
53
54
55



1
2
3
4
5
6
7
8
9
10
11
12
13
14
15
16
17
18
19
20
21
22
23
24
25
26
27
28
29
30
31
32
33
34
35
36

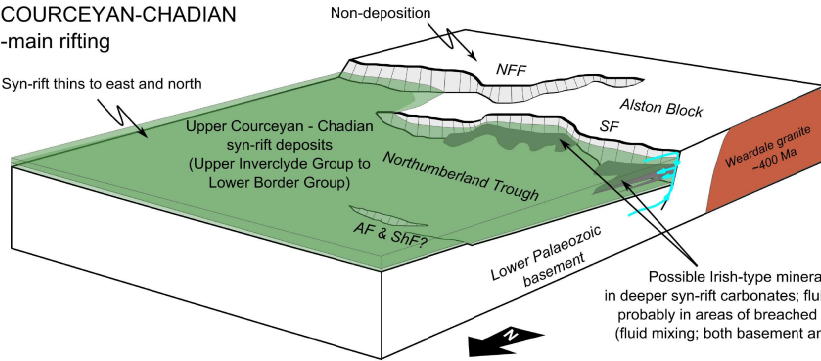
A) COURCEYAN
-early rifting

Late-Devonian - Early Courceyan
pre-rift deposits
(Lower Inverclyde Group)



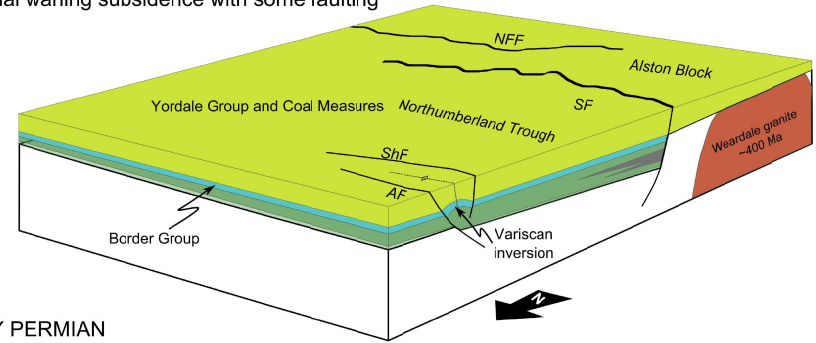
B) COURCEYAN-CHADIAN
-main rifting

Syn-rift thins to east and north
Upper Courceyan - Chadian
syn-rift deposits
(Upper Inverclyde Group to
Lower Border Group)



Possible Irish-type mineralisation
in deeper syn-rift carbonates; fluid entry points
probably in areas of breached relay ramps
(fluid mixing; both basement and seawater)

C) MID-VEISEAN TO END-CARBONIFEROUS
-regional waning subsidence with some faulting



D) EARLY PERMIAN
-renewed regional subsidence and
increased heat flow

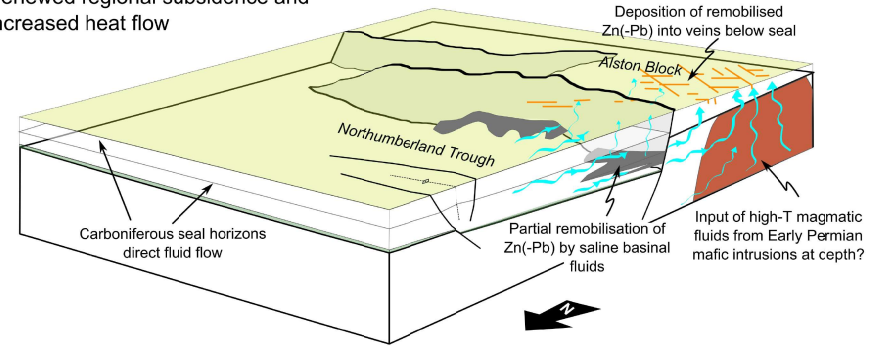


Table 1. Comparison of the known Pb-Zn mineralization in the Irish Midlands and the NPO

	Irish Midlands	NPO
Host lithologies	Shallow water limestones and reef formations	Limestone, sandstone, dolerite (Whin Sill)
Host rock age	Mainly Courceyan	Dinantian and Namurian
Mineralisation style	Sphalerite and galena; replacement of carbonate host rocks at or near palaeo-seafloor (?)	Sphalerite and galena; veining in fractured host rocks, localised replacement of carbonates adjacent to veins
Mineralisation age	Courceyan–Arundian	Early Permian (?)
Tectonic setting	Within or on margins of basin, along major syndepositional faults	Along fractures with small displacement on structurally elevated block
Geodynamic setting	Early stages of basin formation	Associated with Variscan tectonics (?)

60
61
62
63
64
65
66
67
68
69
70
71
72
73
74
75
76
77
78
79
80
81
82
83
84
85
86
87
88
89
90
91
92
93
94
95
96
97
98
99
100
101
102
103
104
105
106
107
108
109
110
111
112
113
114
115
116
117
118

Table 2. Comparison of mineralising feeder faults in Ireland and potential feeder faults in Northumberland

Northumberland Faults	Strike	Max throw at Top Fell Sst (TWT)*	Age
Stublick†	E-W	0.8 s (1800 m)	Lower Carboniferous
Sweethope	ENE-WSW	0.2 s (450 m)	Lower Carboniferous
Causey Park	ENE-WSW	0.05 s (112.5 m)	Unclear
Hallington Reservoir	E-W	0.06 s (135 m)	Unclear
Stobswood (N-dip)	NE-SW	0.05 s (112.5 m)	Unclear
Irish Deposits ‡	Strike	Max throw on feeder faults	Age
Navan	ENE within regional NE-SW trend	500+ m**	Chadian - Arundian
Lisheen	E - ENE within NE-SW regional trend	200 m	Late Courceyan - early Chadian
Silvermines	E-W within NE-SW regional trend	335 m	Late Courceyan
Tynagh	E within NE-SW regional trend	600 m	Late Courceyan - early Chadian

*Converted to meters using $V_p = 4500 \text{ m s}^{-1}$ from Kimbell et al. (1989)

**Navan Fault with the newly discovered Tara Deep satellite deposit in its footwall up to 1 s TWT throw, i.e. >1.5-2km (Ashton et al., 2018)

†Max throw given at the Top Basement reflector; throw at the Top Fell Sandstone reflector is likely significantly lower

‡ Data compiled from Taylor (1984), Shearley et al. (1995), Hitzman (1999), Ashton et al. (2015)